andela.niels@gmail.com
Manuscript prepared for Biogeosciences Discuss.
with version 4.0 of the LaTeX class copernicus_discussions.cls.
Date: 10 April 2013

Global changes in dryland vegetation dynamics (1988-2008) assessed by satellite remote sensing: Combining a new passive microwave vegetation density record with reflective greenness data

Niels Andela[1], Yi Y. Liu[2,4], Albert I.J.M. van Dijk[3,4], Richard A.M. de Jeu[1], and Tim R. McVicar[4]

[1]Earth and Climate Cluster, Department of Earth Sciences, Faculty of Earth and Life Sciences, VU-University, Amsterdam, Netherlands
[2]Water Research Centre, School of Civil and Environmental Engineering, University of New South Wales, Sydney, Australia
[3]Fenner School of Environment & Society, The Australian National University, Canberra, Australia
[4]CSIRO Land and Water, GPO Box 1666, Canberra, 2601, ACT, Australia

Correspondence to: N. Andela
(n.andela@vu.nl)

Abstract

Drylands, covering nearly 30 % of the global land surface, are characterized by high climate variability and sensitivity to land management. Here, two satellite observed vegetation products were used to study the long-term (1988-2008) vegetation changes of global drylands: the widely used reflective-based Normalized Difference Vegetation Index (NDVI) and the recently developed passive-microwave-based Vegetation Optical Depth (VOD). The NDVI is sensitive to the chlorophyll concentrations in the canopy and the canopy cover fraction, while the VOD is sensitive to vegetation water content of both leafy and woody components. Therefore it can be expected that using both products helps to better characterize vegetation dynamics, particularly over regions with mixed herbaceous and woody vegetation. Linear regression analysis was performed between antecedent precipitation and observed NDVI and VOD independently to distinguish the contribution of climatic and non-climatic drivers in vegetation variations. The changes in the persistent and recurrent vegetation signal components were further analyzed using both products. Where possible, the contributions of fire, grazing, agriculture and CO_2 level to vegetation trends were assessed. The results suggest that NDVI is more sensitive to fluctuations in herbaceous vegetation, which primarily use shallow soil water whereas VOD is more sensitive to woody vegetation, which additionally can exploit deeper water stores. Globally, evidence is found for woody encroachment over drylands. In the arid drylands, woody encroachment seems to be at the expense of herbaceous vegetation and a global driver is interpreted. Trends in semi-arid drylands vary widely between regions, suggesting that local rather than global drivers caused most of the vegetation response. In savannas, besides precipitation, fire regime plays an important role in shaping trends. Our results demonstrate that NDVI and VOD provide complementary information, bringing new insights on vegetation dynamics.

1 Introduction

Drylands cover nearly 30 % of the global land surface. They are characterized by high climate variability and are sensitive to land use practice (Tietjen et al., 2010). Here we define *arid drylands* as all areas that have a ratio of long-term mean annual precipitation to mean annual potential evaporation of 0.1 <P/ET$_p$ $\leq$ 0.3 and *semi-arid drylands* as 0.3 <P/ET$_p$ $\leq$ 0.7. Globally the primary drivers of vegetation dynamics in drylands include: (i) climate (Herrmann et al., 2005; Bai et al., 2008); (ii) fire regime (Bond and Keeley, 2005; Archibald et al., 2010); (iii) grazing (Asner et al., 2004; Liu et al., 2013); (iv) agriculture (Piao et al., 2003; Jeyaseelan et al., 2007); and (v) atmospheric CO_2 concentrations (Bond and Midgley, 2012). Fire, grazing and agriculture could be considered to the main land use practices that affect large scale vegetation trends in drylands. Other factors, e.g., nitrogen deposition and changes in growing season length (Bai et al., 2008) may also play an important role locally. Changes in the five primary drivers are expected to result in differential responses of woody cover (i.e., woody encroachment or decline) and herbaceous cover (Archer et al., 1995; Van Auken, 2000; Bond et al., 2003; Asner et al., 2004). Dryland climates generally shows high precipitation variability, increasing the risk of human management altering ecosystems during persistent dry periods (Tietjen et al., 2010; Liu et al., 2013). Bond and Keeley (2005) show that many drylands would be covered by forest rather than grasslands or savannas if fire did not occur frequently. Over the last decades, many dryland ecosystems have faced increased pressure from human demands and climate change (Asner et al., 2004; Dore, 2005; Liu et al., 2012).

Although supporting evidence has been found that each of the five primary drivers can result in responses of dryland vegetation cover, simultaneous changes of the five primary drivers and interactions among them and interaction with ecosystem processes make it difficult to attribute change to any single driver (Bond and Midgley, 2012). Using remote sensing data the evidence of climate impacting vegetation dynamics has been studied at regional (Evans and Geerken, 2004; Herrmann et al., 2005; Wessels et al., 2007), continental (Donohue et al., 2009) and global scales (Nemani et al., 2003). Land use changes - in particular, fire, grazing and

agricultural development - are less well studied. Remote sensing data on global fire regimes are available, with many improved products becoming available since the launch of MODIS in 1999 (Kaufman et al., 1998). Studies of fire induced vegetation change are mainly performed regionally (e.g., Flannigan et al., 2009; Archibald et al., 2010; Heisler et al., 2003) although some notable global exceptions exist (Bowman et al., 2009; Bond et al., 2005). Vegetation indices have been widely used as indicators for advances in agricultural practice (e.g., irrigation and fertilization) and annual crop yields (e.g., Tottrup and Rasmussen, 2004), while land cover maps provide information on the spatial extend of agriculutre. Several studies provide field evidence of the impact of grazing (Van Auken, 2000; Asner et al., 2003) and rising CO_2 levels (McMahon et al., 2010; Buitenwerf et al., 2011) on vegetation cover; however, these studies are regional, presumably to avoid problems of complexity and data availability. Globally, the relative importance and spatial distributions of the five primary drivers (i.e., climate, fire, grazing, agriculture and CO_2) impacting vegetation responses is actively debated (Archer et al., 1995; Asner et al., 2004; Bond and Keeley, 2005; Bond et al., 2005; Fensham et al., 2005; Sankaran et al., 2005; Buitenwerf et al., 2011; Lehmann et al., 2011; Bond and Midgley, 2012).

Satellite remote sensing is a powerful tool to globally study both woody encroachment and desertification, complementing local to regional field evidence and process studies. The Normalized Difference Vegetation Index (NDVI) is the most widely used spectral vegetation index and is based on a ratio of red and near infrared reflectance (Rouse et al., 1974; Tucker, 1979; Beck et al., 2011). NDVI has been used as an indicator of vegetation productivity (Tucker et al., 1985); and is related to Leaf Area Index (LAI; Wang et al., 2005), canopy cover fraction and the fraction of absorbed photosynthetically active radiation (fPAR; Asrar et al., 1984; Carlson and Ripley, 1997; Lu et al., 2003). Complementary to the NDVI, a recently developed dataset is Vegetation Optical Depth (VOD). VOD describes the transparency of vegetation in the microwave domain and is mostly sensitive to vegetation water content (Kirdiashev et al., 1979). Owe et al. (2001) developed the Land Parameter Retrieval Model (LPRM) to derive VOD from low frequency passive microwave observations. This model was further improved by Meesters et al. (2005) and has been applied to microwave data observed by the Nimbus-7 SMMR, DMSP

SSM/I, TRMM TMI, and Aqua AMSR-E sensors to estimate both soil moisture and VOD (Owe et al., 2008). VOD is sensitive to vegetation water content in both the woody and leafy vegetation components, and is therefore a good indicator for above-ground biomass (Liu et al., 2011a).

Due to the different characteristics of reflective and microwave satellite remote sensing, NDVI and VOD exhibit differential responses to vegetation dynamics (Shi et al., 2008). NDVI does not penetrate vegetation and thus saturates at a certain level of leaf cover (Tucker, 1979). As a consequence, temporal correlation between NDVI and VOD is high for grass and croplands but lower for high biomass vegetation types where NDVI saturates (Liu et al., 2011a). Both reflective and microwave products have been used to study vegetation dynamics. Pettorelli et al. (2005) reviews ecological studies that used NDVI; it has been used to study climate- and human-induced vegetation change (e.g. Evans and Geerken, 2004; Herrmann et al., 2005; Wessels et al., 2007), global vegetation trends (e.g. de Jong et al., 2011; Fensholt et al., 2012) and land degradation (e.g. Bai et al., 2008). Long VOD time series were only recently developed, and so far have been used to study vegetation phenology (Jones et al., 2011, 2012) and to show the impact of El Niño Southern Oscillation on Australian vegetation cover (Liu et al., 2007). Global trends in VOD were shown to correspond to changes in precipitation, livestock (e.g., overgrazing), crop production, deforestation and fires (Liu et al., 2012, 2013).

To date, only one study assessed trends in NDVI and VOD together, and did so only in an introductory manner (Liu et al., 2011a). It found many regions with similar trends but also regional differences, and illustrated that VOD provides new information for mixed woody-herbaceous land cover types. Detailed analysis of the driver-response relationships of the complementary NDVI and VOD responses was not conducted (Liu et al., 2011a). Due to the characteristics of both products, differential responses in mixed woody-herbaceous land cover types are expected. Compared to VOD, NDVI saturates at relatively low biomass and is therefore most sensitive to vegetation covering the largest surface (Liu et al., 2011a). Grasses are the main source of large interannual variation in NDVI for savanna ecosystems (Archibald and Scholes, 2007; Roderick et al., 1999b; Lu et al., 2003; Donohue et al., 2009). VOD has a greater penetration capacity

and is associated with total above-ground biomass, therefore VOD is more sensitive to changes in woody vegetation (Liu et al., 2011a; Shi et al., 2008). The relationship between NDVI and VOD is further explored in the background theory section.

This paper uses the two complementary remote sensing datasets and analyzes their trends across the global drylands. Differences between NDVI and VOD are explored and trends are interpreted from an ecological perspective. A model is developed to predict the vegetation responses that can be accounted for by precipitation variation. Residual trends (i.e., the observed minus model-explained trends) and their potential drivers are discussed and attributed, where possible, using global data on burned area, grazing and literature. Despite the limited data availability on the drivers associated with land use; we find that information on regional ecosystems (e.g., land cover type and water availability) in combination with knowledge of grazing intensity and burned area time series can provide important information on trends in vegetation density and composition. To date, the impact of grazing and fire have not been included in global studies of dryland vegetation dynamics (e.g. Nemani et al., 2003; Fensholt et al., 2012; de Jong et al., 2011). We address the following questions:

1. How do NDVI and VOD complement each other and what do combined trends tell us about vegetation dynamics?
2. What component of temporal dryland vegetation dynamics is explained by precipitation?
3. What are the remaining trends in both vegetation indices, and how are they related to the other primary drivers (fire, grazing, agriculture and CO_2)?

The results elucidate changes in global dryland biomass and composition, and provide a spatially explicit analysis across the globe of previously primarily locally applied conceptual frameworks.

2 Background theory

Herein, a conceptual framework is developed to relate temporal patterns and trends in NDVI and VOD to vegetation characteristics. In relation to NDVI, the optical reflectance observations from which it is derived can be thought of as a linear mixture of the respective reflectance of the constituent surface components:

$$\rho = f_o\rho_o + (1 - f_o)(f_u\rho_u + f_s\rho_s) \quad (1)$$

where ρ is reflectance in the wavelength considered, f the fraction canopy cover, and the subscripts denote overstory (o), understory (u) and soil surface (s). Homogeneous vegetation cover is assumed such that the overstory will obscure some part of the understory, and it is assumed that the NDVI observations are representative for nadir measurements such that f equates to projected canopy cover. NDVI is calculated as a reflectance difference index. As a consequence it can be shown theoretically (using equation 1) that NDVI will respond to surface component mixing ratios in a slightly non-linear manner although NDVI still converges to end member NDVI values when these dominate overall reflectance (Asner, 1998). Although there is not necessarily a consistent difference between overstory and understory NDVI over the world's drylands, NDVI per unit canopy area for recurrent vegetation tends to exceed that of persistent vegetation. Because the NDVI is responsive to leaf chlorophyll concentration, this may be interpreted as a result of functional convergence between leaf chlorophyll, structural properties, leaf life span and life form, with recurrent vegetation having shorter-lived and 'greener' leaves (Reich et al., 1997, 2003). As a result, all else being equal, an increase in NDVI can be explained by an increase in total canopy cover or a relative increase in recurrent vegetation canopy cover, or both. It is noted that in drylands, recurrent and persistent vegetation components will often correspond to herbaceous and woody vegetation (Roderick et al., 1999b; Lu et al., 2003; Donohue et al., 2009), though not always: both recurrent woody vegetation (e.g., deciduous trees) and persistent non-woody vegetation (e.g., succulents) exist. By the same token, woody vegetation can exist in the understory.

VOD (denoted τ) can be interpreted as being linearly related to total above-ground biomass (AGB) water content, i.e., the sum of water in woody and non-woody vegetation (Jackson et al., 1982; Wigneron et al., 1993):

$$\tau = \tau_o + \tau_u = c_\tau(\theta_o m_o + \theta_u m_u) \tag{2}$$

where θ is vegetation water content, m the AGB, and c_τ the constant of proportionality. Fresh biomass water content θ will normally be greater for herbaceous vegetation than for woody vegetation (Roderick et al., 1999a, 2000). Therefore, an increase in VOD can mean an increase in total AGB, an increase of the fraction of herbaceous vegetation AGB, or both.

Finally, the relationship between NDVI and VOD is influenced by the connection between AGB (m) and canopy cover (f). This relationship can be presented by considering the commonly used light extinction equation (Monsi and Saeki, 2005) that relates f to leaf area index (Λ):

$$f = 1 - \exp(-\kappa\Lambda) = 1 - \exp(-\kappa\alpha_{SLA} f_{leaf} m) = 1 - \exp(-c_\Lambda m) \tag{3}$$

where κ is the extinction coefficient, α_{SLA} the specific leaf area (i.e., area per unit leaf mass), and f_{leaf} the fraction of leaf biomass in total AGB. While κ depends on leaf orientation and clumping, f_{leaf} and α_{SLA} will be greater for non-woody vegetation than for woody vegetation. Overall, total AGB remaining unchanged, the sensitivity of NDVI to a relative increase in the herbaceous component is expected to be considerably greater than the sensitivity of VOD. VOD, being sensitive to AGB water content, is expected to be more sensitive to a relative increase in woody vegetation. Although per unit mass, the tree foliage will have a somewhat higher relative water content than the woody parts, woody biomass typically represents 90% or more of total above-ground biomass (Northup et al., 2005, and references therein) and also contains most of the water (Sternberg and Shoshany, 2001). The above considerations lead to the following four expectations:

1. an increase in both NDVI and VOD signifies an increase in the herbaceous biomass component and/or an increase in total AGB;

2. an increase in NDVI combined with a decrease in VOD signifies an increase in the herbaceous component;

3. a decrease in NDVI and an increase in VOD signifies an increase in the woody component; and

4. a decrease in both NDVI and VOD signifies a decrease in the herbaceous biomass component and/or a decrease in total AGB.

3 Materials

In order to study global long-term dryland vegetation dynamics, both NDVI and VOD datasets were used for their overlapping period 1988-2008. Both vegetation indices are dimensionless and in this study we use a 0.25° spatial and monthly temporal resolution. Key characteristics of the datasets are illustrated in Fig. 1.

3.1 Normalized Difference Vegetation Index (NDVI)

The NDVI data used were from the Global Inventory Modeling and Mapping Studies 3^{rd} generation (GIMMS3g) data product derived from the Advanced Very High Resolution Radiometer (AVHRR) sensor on board the NOAA series of satellites (i.e., NOAA 7,9,11,14,16 and 17; Tucker et al., 2005). The data were resampled from 1/12° to 0.25° spatial resolution and from twice to once monthly temporal resolution by simple averaging. Data were available between 1981-2010. Recently Beck et al. (2011) showed that of four AVHRR processing chains tested, GIMMS was best able to track trends in 1,424 Landsat image pairs. Sensor characteristics and atmospheric variations introduce uncertainty in the NDVI signal over non-vegetated surfaces, including snow and ice (Brown et al., 2006).

3.2 Vegetation Optical Depth (VOD)

Liu et al. (2011a) harmonized different VOD datasets from different sensors derived from LPRM into one consistent time series. The Cumulative Distribution Function (CDF) matching technique was applied to merge the VOD products, with AMSR-E VOD data used as the reference dataset. This rescaling technique did not affect the relative dynamics of the original products (Liu et al., 2011b), and resulted in a monthly 0.25° resolution dataset from 1988 to 2008. AMSR and TRMM VOD datasets are available through the NASA Mirador data Portal (ftp://hydro1.sci.gsfc.nasa.gov/data/s4pa/WAOB/) and SMMR and SSM/I VOD is available upon request. The accuracy of the VOD products is within the order of 0.04 and retrievals are less reliable over disiccated loose soil as found in sand deserts (de Jeu, 2003). Moreover, VOD values are sensitive to frost conditions and open water (Jones et al., 2011; Gouweleeuw et al., 2012).

3.3 Additional datasets

Precipitation data (monthly; 1901-2009) produced by the University of East Anglia Climatic Research Unit (CRU) were available at a 0.5° resolution (http://badc.nerc.ac.uk/view/badc.nerc.ac.uk__ATOM__dataent_1256223773328276; Jones and Harris, 2008). For analysis it was assumed that within this grid cell precipitation was homogeneously distributed and data was resampled to a 0.25° resolution.

The MODIS Land Cover Type Yearly Climate Modeling Grid (MCD12C1; 2005; 0.05° resolution), land cover map was used here (https://lpdaac.usgs.gov/products/modis_products_table/land_cover/yearly_l3_global_0_05deg_cmg/mcd12c1; NASA, 2008). Data was resampled to a 0.25° resolution using the land cover with the highest frequency in each grid cell. The land cover types follow the University of Maryland (UMD) classification scheme (Hansen et al., 2000). For our analysis some land cover classes were merged to assist interpretation (i.e., urban and built-up, barren or sparsely vegetated, and unclassified + fill were here merged into 'barren or sparsely vegetated'; all types of forest into 'forest'; and closed and open shrublands into

'shrublands').

Monthly burned area data was available based on MODIS Terra satellite imagery (MCD64A1; 500m resolution; Nov./2000 onwards Giglio et al., 2009). Data was rescaled to a monthly 0.25° resolution by calculating the mean burned area per 0.25° grid cell.

Livestock density was available from the Food and Agriculture Organization's (FAO) Gridded Livestock of the World data (http://www.fao.org/AG/againfo/resources/en/glw/GLW_dens.html; Robinson et al., 2007) and was expressed in Tropical Livestock Units (TLU) per km^2 (1 TLU = 250 kg live weight, cattle = 0.7 TLU, sheep and goats = 0.1 TLU; Jahnke, 1982). The FAO livestock density data has a spatial resolution of 0.05° and is not temporally varying hence time series analysis of this driver could not be performed.

4 Methods

4.1 Relationship between NDVI and VOD

After exploring the relation between NDVI and VOD in a theoretical manner in Sect. 2, we calculated mean values of NDVI and VOD for each month of the year and compared seasonal patterns for grasslands, savannas and woody savannas of southern Africa. Annual mean values and range (maximum minus minimum value) were also calculated and compared for the three selected land cover types with increasing woody cover. The results of this analysis were used to verify the four expectations of Sect. 2, regarding the co-relationships between NDVI and VOD. Trends in NDVI and VOD were analyzed separately as described in section 4.2 and 4.3, but co-trends in NDVI and VOD were also interpreted using our theoretical framework.

4.2 Response of vegetation index anomalies to antecedent precipitation anomalies

Nicholson et al. (1990) found a linear relationship between NDVI and precipitation for regions in northern and east Africa with precipitation below 1000 mm yr^{-1}. In some other areas, satu-

ration effects during the wet season occurred at lower thresholds depending on local conditions like soil type (Nicholson and Farrar, 1994). Most of the drylands (93 %), as defined here receive less precipitation than 1000 mm yr^{-1}, and remaining areas are characterized by high potential evaporation (i.e., ET$_p$ >1430 mm yr^{-1}). Following Evans and Geerken (2004) and Herrmann et al. (2005) a linear model therefore used. Linear regression models between antecedent precipitation and each vegetation index were developed for each grid cell. These regression models were used to estimate the long-term vegetation trends expected due to precipitation patterns alone. Expected vegetation trends were calculated in three steps. Firstly, the mean seasonal cycle in vegetation index d was removed to produce anomalies:

$$d'(t) = d(t) - \overline{d}(m). \tag{4}$$

Where $d'(t)$ is the anomaly for month (t), $d(t)$ is the original data and $\overline{d}(m)$ is the average value for each specific month (m) in the time series. Anomalies were calculated both for precipitation and the vegetation products (NDVI and VOD). Second, the antecedent precipitation index (API) was calculated, here defined as the optimal correlating precipitation running mean (PRM) as judged from Spearman's ranked correlation coefficient (R_s) over 1 to 60 month averaging periods. The $API(x,y,t)$ was calculated for each grid cell (x,y) and month t using:

$$API(x,y,t) = \frac{\sum_{t-(T(x,y)-1)}^{t} d'(x,y,t)}{T(x,y)}. \tag{5}$$

Where T is the averaging period in months for antecedent precipitation that leads to the highest R_s between the PRM and the vegetation anomalies (NDVI or VOD). The expected vegetation variation was calculated using as a linear function of API:

$$expected(x,y,t) = a_1(x,y) * API(x,y,t) + a_2(x,y). \tag{6}$$

For each grid cell the coefficients a_1 and a_2 were determined by least squared differences between the API and vegetation anomaly time series. The residual trend was calculated as the observed minus expected trend and represents the component of the signal that could not be directly attributed to precipitation variations. Similar approaches were used by Evans and Geerken (2004), Herrmann et al. (2005) and Wessels et al. (2007) for NDVI, who also assumed (as we do) that if vegetation variation expected on the basis of precipitation variation was removed from observed vegetation anomalies, the residual trends are largely independent of precipitation. Here we used a model based on precipitation and vegetation anomalies rather than the original vegetation indices. Because all trends are present in the anomalies, and not in the seasonal pattern, a model optimized to follow anomalies will give a better estimation of trends in the vegetation indices caused by precipitation. Although direct correlation between precipitation and vegetation indices will be higher than correlation between vegetation index and precipitation anomalies, a model based on the original vegetation indices and precipitation will be more useful to study the effect of precipitation on seasonal rather than interannual vegetation dynamics. To facilitate comparison with published studies, the analysis was also repeated using the original vegetation indices rather than anomalies (cf. Herrmann et al., 2005).

Grid cells with less than 40% valid data (i.e., 100 or less of the 252-month series) in either vegetation dataset were not included in this analysis. NDVI cannot be used over snow and ice (Brown et al., 2006), while VOD is sensitive to frost conditions (see Sect. 3.2; Liu et al., 2011a), hence seasonally recurrent data gaps exist in both products during wintertime. This relatively low threshold of 40% valid data was chosen in order to include most drylands at high latitudes/elevations. Data gaps have been ignored in trend calculations but are considered in their interpretation.

4.3 Global dryland vegetation trends

We expect that climate and land cover affect NDVI and VOD dynamics and may cause them to respond differently to the primary drivers of dryland vegetation dynamics. Hence, to stratify our

results, we used global maps of land cover (Fig. 1a) and P/ET_p classes; referred to as humidity classes hereafter (Fig. 1b).

In addition to annual mean NDVI and VOD patterns, seasonal patterns provide extra information about vegetation composition and changes in dominant components. Persistent, or evergreen vegetation is active year-round and shows limited seasonal variation. For most drylands, the main component of persistent vegetation is woody. On the other hand, recurrent vegetation shows a strong seasonal cycle, mainly caused by herbaceous vegetation (Donohue et al., 2009; Lu et al., 2003; Roderick et al., 1999b). A diagram representation of this model is shown in Fig. 2a (cf. McVicar and Jupp, 1998). In reality, deciduous dryland forests exist, and less pronounced canopy cycles can still occur in non-deciduous trees, therefore a residual seasonal phenology in the woody component has been proposed, resulting in models similar to Fig. 2b (cf. Donohue et al., 2009; Lu et al., 2003). The opposite situation can also occur: part of the herbaceous vegetation can be evergreen (Roderick et al., 1999b).

We implemented the model represented in Fig. 2a as there is no single preferable solution globally for Fig. 2b; local ecological conditions will determine the differential and combined responses from the woody and herbaceous vegetation. Long-term linear trends of the two separate components of the vegetation indices, i.e., the annual minimum values and the residual signal (i.e., annual mean minus minimum) were calculated. We hypothesize that these two components provide information on changes in the evergreen and seasonally recurrent vegetation components respectively, in the case of NDVI (Donohue et al., 2009); and in the woody and herbaceous vegetation components respectively, in the case of VOD. Further on, this will be demonstrated by comparing seasonal patterns of NDVI and VOD for southern African grasslands, savannas and woody savannas (see results).

Global maps of livestock density, burned area, recent trends in burned area, and ecosystem characteristics of land cover and humidity were used to interpret results. It was assumed that globally consistent trends not explained by climate, fire, grazing and agricultural developments

might be caused by increasing atmospheric CO_2 concentrations (Bond et al., 2003). Per grid cell time series of NDVI, VOD and burned area were used to explore impact of fire on vegetation indices. A conventional non-parametric Mann-Kendall trend test was used to determine areas of significant monotonic trends (cf. de Jong et al., 2011; Fensholt et al., 2012; Liu et al., 2012). Only results significant at $p<0.05$ are shown unless indicated otherwise. The non-parametric Theil-Sen estimator of slope is insensitive to outliers and was used to calculate linear trends (Sen, 1968; Theil, 1950).

5 Results

5.1 Relationship between NDVI and VOD

In order to verify the four expectations of the background theory (Sect. 2), characteristics of three land cover types of southern Africa were studied (study areas are shown in Fig. 3d). With increasing woody cover (i.e., along the gradient from grassland in the south through savanna to woody savanna in the north), VOD increased faster than NDVI (Fig. 3a, b and c). The annual average VOD for grassland was 0.41 and for woody savanna this increased to 0.70 (i.e., a 0.29 increase). In contrast the annual average NDVI only increased 0.19 (i.e., from 0.43 for grassland to 0.62 for woody savanna). However, the NDVI range (annual maximum minus minimum) is exceeding the VOD range for all three land cover types (Fig. 3a, b and c).

5.2 Response of vegetation index anomalies to antecedent precipitation anomalies

The strongest correlation (R_s) between vegetation anomalies and antecedent precipitation index (API) were observed over arid drylands ($0.1 < \mathrm{P/ET}_p \leq 0.3$; Fig. 4a and c). While NDVI and VOD showed similar spatial patterns, VOD showed higher correlation coefficients, suggesting that VOD reacts stronger to interannual precipitation variability in drylands than NDVI. In regions with low or insignificant correlations between vegetation and API, factors other than precipitation are likely to determine interannual vegetation variability and/or variability was minimal over the study period. While for most land cover classes VOD had larger areas with

significant correlations, NDVI was more responsive to changes in croplands (Table 1).

Averaging periods (denoted T in the methods; Fig. 4b and d) are related to the capacity of vegetation to use antecedent precipitation and the lead time of interannual variation in precipitation followed by a vegetation response. NDVI generally has shorter averaging periods than VOD. To facilitate comparison with other studies, model results based on original vegetation indices and precipitation are shown in the annex material (Fig. A.1). In general, observed correlation was higher, and averaging periods were shorter for the model based on original vegetation indices and precipitation (Fig. A.1) compared to the model based on anomalies used here (Fig. 4, see Sect. 4.2). Figure 5 shows box plots of the data in Fig. 4, stratified by land cover and humidity classes. Both NDVI and VOD showed longest averaging periods for areas dominated by woody vegetation and croplands, shorter periods were observed for grasslands and savannas.

Figure 6 shows an example of expected and observed anomalies in NDVI and VOD for two $5^\circ \times 5^\circ$ regions (Fig. 3d), in eastern Australia (25-30°S, 145-150°E) and in southern Africa (25-30°S, 20-25°E). Modeled NDVI is based on shorter averaging periods, because the signal showed little interannual variation. VOD, on the other hand, is usually based on longer averaging periods and therefore follows the interannual variation in precipitation, ignoring small intra-annual variability.

5.3 Global dryland vegetation trends

Figure 7a and b show observed annual trends in NDVI and VOD (1988 - 2008). Some regions showed similar trends in both datasets: e.g., India, Mongolia, North America, eastern Australia, and northern African savannas. Other areas showed contrasting trends between the datasets: e.g., southern Africa, northern Australia, Argentina and central Asia. While global trends in NDVI and VOD differ considerably, the expected trends in NDVI and VOD were relatively similar and strong decreasing trends were found in southeastern Australia and Mongolia, while increasing trends were found in most of Africa and northern Australia (Fig. 7c and d). Figure 7e and f show residual trends, calculated as observed anomalies minus expected vegetation anoma-

lies. For the NDVI (Fig. 7e) some trends persisted (e.g., positive trends over most of India and Spain, and negative trends over southern Russia and Kazakhstan). In other cases, if observed and expected trends had the opposite direction (i.e., one is positive and the other negative) this resulted in enhanced residual trends (e.g., Argentina, arid northern Africa, southern Africa and northern Australia in the case of NDVI; compare Fig. 7a, c and e). If observed and expected trends had the same direction this resulted in weakened residual NDVI trends (e.g., Mongolian steppe and semi-arid drylands of northern Africa), or trends tended to zero (e.g., southern India and northern China). Finally, in some regions new NDVI trends emerged (southeastern Australia and south-west Western Australia). Observed and expected trends in VOD generally had the same direction, resulting in weakened residual trends (e.g., northern Australia, Sahel, southern Africa and southern Argentina; compare Fig. 7b, d and f). Although there were also regions with observed trend in VOD, but no trends in expected vegetation anomalies (e.g., east Africa and northern India).

Box plots of the distribution of observed, expected and residual trends, stratified by land cover and humidity classes, illustrate that NDVI overall had less distinct trends than VOD (Fig. 8). Median observed trends in NDVI were increasing for savanna and croplands, and decreasing for the other land cover classes (Fig. 8a). For VOD decreasing median observed and residual trends were found in forested drylands, while increasing median trends were found for all other land cover classes (Fig. 8a and c). Over arid drylands the median VOD trend was increasing while NDVI showed mostly decreasing trend; for more humid drylands NDVI and VOD trends were more similar and closer to zero. Savannas and shrublands showed a small increase in expected median NDVI and VOD (Fig. 8b), indicating that part of the change in median vegetation index response is explained by trends in precipitation. In the residual trends (i.e., observed minus expected) similar patterns remained, both for NDVI and VOD (Fig. 8c and f). For NDVI, the increasing trend in savannas declined when comparing the observed and residual trends (Fig. 8a and 8c, respectively) while the decreasing median trends in bare or sparsely vegetated regions, shrublands and grasslands remained when comparing the observed and residual trends (i.e., compare the NDVI results for B/SV, Sh and Gr in Fig. 8a with 8c). Because of the removal

of the vegetation response expected due to precipitation variation, the residual trends were generally smaller then observed trends (i.e., compare Fig. 8a with 8c and Fig. 8d with 8f). There were no particular humidity classes that showed a large change in expected median vegetation, indicating that median changes in precipitation were close to zero for each humidity class (Fig. 8e).

Trends in annual time-step minimum NDVI values were decreasing throughout most drylands (Fig. 9a), suggesting a decline in evergreen vegetation in those regions. However, some areas (e.g., northern Australia and parts of sub Sahara Africa) showed rising minimum VOD values (Fig. 9c) together with declining minimum NDVI (Fig. 9c). Trends in annual mean minus annual minimum NDVI (Fig. 9b), interpreted as the seasonally recurrent vegetation component, were increasing for nearly all areas that showed decreasing trends of minimum values (compare Fig. 9a and b). Minimum VOD trends were increasing in most global drylands (e.g., Africa, Australia and India; see Fig. 9c), while little trend was found in recurrent VOD; however, some strong declines are seen in southeast Australia and the Mongolian steppe (Fig. 9d). Trends in both products were also present at high latitudes (i.e., $>50^{\circ}$), but those results need to be treated with some caution since both products lack winter values if snow cover is present, and early or late snow presence could therefore affect the annual minimum values.

Vegetation trends (Fig. 7 and 9), are expected to be related to trends in precipitation (Fig. 10a) and trends in annual burned area (Fig. 10b). Most global drylands experienced stable or increasing precipitation amounts during 1988-2008; notable exceptions are southeast Australia, the Mongolian steppe and northern China (Fig. 10a). Trends in annual burned area declined for northern Africa and increased in most of southern Africa (Fig. 10b). Southern America showed a mixed pattern of increased and declined trends of annual burned area, while trend of annual burned area over most of Australia has been stable or declined. The relationship between burned area and vegetation indices was further analyzed using three study areas with different land cover in southern Africa. Locations of the study areas are shown in Fig. 3d. For grasslands, annual burned area is relatively low and no obvious relationship between vegetation

indices and burned area is present (Fig. 11a). In savannas, both NDVI and VOD are strongly related to interannual variation in burned area (Fig. 11b; compare 2006 and 2008 with the other years). For woody savannas, increased annual burned area together with relatively low annual minimum NDVI values were observed in 2004 and 2007-2009, but interannual variation was much smaller.

6 Discussion

6.1 Relationship between NDVI and VOD

Our conceptual framework resulted in four expectations corresponding to the four categories of Fig. 12. In addition to exploring the relation between NDVI and VOD theoretically, evidence supporting these expectations was found by comparing grasslands, savannas and woody savannas in southern Africa (Fig. 3a,b and c). It was shown that with increasing biomass and woody vegetation VOD increased faster than NDVI, while NDVI is more sensitive to seasonal greening in regions dominated by herbaceous vegetation. As expected, the seasonal biomass fluctuations seem to be better captured by the VOD signal. Ovington et al. (1963) show that seasonal AGB variation (mostly caused by herbaceous vegetation and tree leaves) for savanna vegetation is about three times larger than for grassland. NDVI range for grasslands (0.20) is nearly as large as NDVI range for savannas (0.26; a 30% increase); while VOD range changes from 0.09 to 0.20 from grassland to savanna (a 120% increase), respectively (Fig. 3a and b).

The co-relationship of NDVI and VOD trends (Fig. 12) provides new insights in the relative performance of herbaceous and woody vegetation components in global drylands. Woody encroachment into grassland or savannas has been observed in many regions across the globe, including Argentina (e.g., Adamoli et al., 1990), Africa (e.g., Vegten, 1984) and Australia (Fensham et al., 2005) and reviewed by Archer et al. (2001). Although satellite observations of NDVI and VOD confirm our theoretical framework, future validation studies, comparing satellite observations with local to regional field studies, can improve regional interpretation and

confidence. Vegetation trends will be discussed in greater detail in Sect. 6.3 for arid and semi-arid drylands separately.

6.2 Response of vegetation index anomalies to antecedent precipitation anomalies

As expected, arid drylands showed strongest correlation between the vegetation index anomalies and API (i.e., median R_s NDVI >0.3, median R_s VOD >0.5; see Fig. 5). Nemani et al. (2003) mapped these areas as being water limited, and for higher latitudes, water and temperature limited. Correlation is less strong than found by some other studies (e.g., Herrmann et al., 2005) or when analyzing the original indices (cf. Fig. A.1) because seasonal vegetation – precipitation responses are not included. In semi-arid drylands, like the savannas of Africa and Australia, regions that have a strong seasonal precipitation response do not necessarily show a strong interannual response (compare Fig. 4a and c with A.1). This could be explained by a seasonal abundance of water in which variation in precipitation does not affect vegetation followed by a dry season in which the vegetation is unable to use antecedent precipitation. Optimum precipitation averaging periods differ considerably for NDVI and VOD (Fig. 4 and 5) and are larger than found if the seasonal cycle is included, rather than the anomalies only (compare Fig. 4 with Fig. A.1). The model based on original vegetation indices and precipitation is mostly affected by short-term vegetation - precipitation response; here, we use a model based on anomalies, that is sensitive to the long-term capacity of vegetation to use antecedent precipitation. Differences between NDVI and VOD are likely observed because they are sensitive to different components of vegetation cover (Fig. 3a, b and c); NDVI is more sensitive to changes in the shallow rooted herbaceous understory (Archibald and Scholes, 2007), and VOD more sensitive to changes in the woody overstory, which can also utilize moisture from deeper soil and groundwater stores (Rossatto et al., 2012; House et al., 2003). The stronger correlations between VOD and API are attributed to the larger interannual variation in the VOD dataset and caused by interannual precipitation variations (Fig. 6). Archibald and Scholes (2007) reported similar findings, and concluded that plants that access deeper water and have carbohydrate reserves may show a phenology that is quite different from surrounding areas with grass cover that depend on shallow soil moisture for their growth. It appears that similar conclusions may be drawn for interannual

variation.

Following previous studies (Evans and Geerken, 2004; Herrmann et al., 2005; Nemani et al., 2003; Wessels et al., 2007; Donohue et al., 2009), we also found that not all interannual variation can be explained by precipitation alone. Although VOD generally shows longer averaging periods than NDVI, spatial patterns in both vegetation indices are quite similar; regions with relatively long averaging periods for one of the vegetation indices are likely to show relatively long averaging periods for the other vegetation index. However, local differences between both vegetation indices are also found (compare Fig. 4b and d). Each vegetation index separately shows local patterns with sometimes sharp changes and some regions showed considerably longer averaging periods than others (seen as rapid changes in color within each of Fig. 4b and d). This particularly occurs in areas of weak correlation between API and vegetation indices. However, some regions (e.g., west Australia and southern Africa) show strong correlation and large local differences in averaging periods, this seems to be due to the presence (or absence) of large interannual variation in precipitation. Distinct local patterns suggest that physical landscape aspects, including landform and soil type, may also contribute.

6.3 Global dryland vegetation trends

Vegetation trends of the world's arid drylands and semi-arid drylands are discussed in turn. Overall, the world's drylands show a decrease in NDVI and an increase in VOD (Fig. 8d).

Arid drylands ($0.1 < \mathbf{P/ET}_p \leq 0.3$)

The world's arid drylands are mainly covered by shrublands (48.2%) and grasslands (31.3%). Trends over bare or sparsely vegetated areas (10.6%) need to be treated with care due to the limitations of both vegetation indices over those regions (see Sect. 3; and Huete et al., 1985; Brown et al., 2006). Arid drylands are characterized by little to moderate rainfall (100 to 600 mm per year) with high interannual variability.

Many arid drylands experienced unchanged or increasing annual precipitation (Fig. 10a), and median expected trends in both vegetation indices were close to zero (Fig. 8e). NDVI median trend for arid drylands was negative while VOD median trend was positive (Fig. 8e). Both the relatively constant or increasing VOD trends and most negative trends in NDVI remain after precipitation induced variation is accounted for (Fig. 7e and f). This results in many regions showing opposite trends in NDVI and VOD (Fig. 12; e.g., arid drylands of Argentina, southern Africa, northern Africa and Australia). In those regions, it seems that woody encroachment takes place at the expense of the herbaceous understory. Woody versus herbaceous vegetation shifts have previously been attributed to climate (Fensham et al., 2005), fire regime (Sankey et al., 2012), grazing (Asner et al., 2004) and CO_2 fertilization (Buitenwerf et al., 2011).

Clear trends in the residual NDVI and VOD indicate that next to precipitation, other drivers also play a role (Fig. 7e and f). A possible explanation for residual trends could be changing fire regimes (Fig. 10b) through its impact on competitiveness of the herbaceous and woody vegetation components (Sankey et al., 2012). Bowman et al. (2009) showed that annual burned area is highest in areas of intermediate primary production, limited by a lack of dry periods towards the tropics and limited by a lack of fuel towards dry areas (Fig. 10d). Primary production is the main limitation on annual burned area in these drier regions (Archibald et al., 2009). This results in a system of highly variable biomass production, followed by infrequent fires (Fig. 11a). Increasing precipitation is expected to increase annual burned area in arid drylands. Increased burning can impact dry season minimum NDVI values (Fig. 11; Díaz-Delgado et al., 2003) and suppress woody encroachment (Lehmann et al., 2011). However, recent (2000-2011) trends in annual burned area do not show increases in most arid drylands and showed declines in northern Australia and the Sahel (Fig. 10b). This, combined with an average annual burned area of below 10% (Fig. 10d), seems to make fire an unlikely driver of globally observed changes.

Decreasing NDVI trends have been interpreted as a proxy for land degradation (Wessels et al., 2007; Bai et al., 2008) which might be caused by grazing. Grazing has also been associated with woody encroachment (e.g., Asner et al., 2004). Although grazing might cause contradict-

ing trends between NDVI and VOD in some regions (e.g., arid parts of northern Africa) similar trends are observed in regions of limited or no grazing by domestic livestock (e.g., compare Fig. 10c and 12 for arid drylands of Argentina and Australia). The spatial patterns and scale at which trends occur suggest that grazing by domestic livestock is not the main driver in these cases, impact of grazing by non-domesticated animals was not included here, as no information was available to us.

Sankaran et al. (2005) suggest that woody vegetation receiving less than 350 mm annual precipitation is largely constrained by water availability. Rising atmospheric CO_2 concentrations affects water use efficiency and photosynthetic rates as well as light and nutrient efficiency (Drake et al., 1997; Farquhar, 1997). CO_2 is reported to enhance the relative performance of woody C3 species over the C4 grasses that dominate tropical savannas (Bond and Midgley, 2012; Higgins and Scheiter, 2012). Once woody plants are established in savannas, they are likely to limit the growth of herbaceous plants by water uptake and shading (Breshears, 2006).

Increases in extreme air temperatures and changes in growing season duration can also explain some of the observed vegetation trends (Allen et al., 2010). Changing duration of rain seasons can impact the relative performance of different species: a shorter but more intense wet season is likely to result in decreasing herbaceous understory (NDVI) during dry seasons, while deep rooted vegetation suffers less, having access to deeper water resources and therefore being more sensitive to long-term water availability (Fig. 5; Archibald and Scholes, 2007). Evidence for shortening growing seasons is found for arid drylands of northern Africa (de Jong et al., 2011). Tietjen et al. (2010) argue that grasses lose competitive strength under decreasing soil moisture resulting in thickening woody vegetation comprised of shrubs. Other possible explanations could be shifts in grass types, both affecting NDVI values directly and changing fire regimes (Brooks et al., 2004). Finally, increased air temperatures can result in higher evaporation rates and during the dry season result in a competitive advantage of deep rooted species over shallow rooted species. Although air temperature is increasing over many drylands globally, decreasing trends are also observed in some regions, as temperature tends to be strongly related

to precipitation through the effect of cloud cover on solar irradiation. Additionally, decreases in wind speed ('wind stilling'), and changes in other meteorological variables governing the evaporative process, also alter the evaporative regime (McVicar et al., 2012). Following Higgins and Scheiter (2012), we suggest that the effects of changing evaporation rates in drylands are less important than the effects of increasing atmospheric CO_2 concentrations. Given that patterns in the residual trends are found in most global arid drylands, all experiencing very different fire and grazing conditions (compare Fig. 7e and f with Fig. 10c and d), a global driver such as CO_2 fertilization may be more plausible.

Semi-arid drylands ($0.3 < P/ET_p \leq 0.7$)

The world's semi-arid drylands mainly contain croplands (26.4%), grasslands (25.0%), savannas (15.9%), forest (15.2%) and woody savannas (12.4%). In southern America, Africa and Australia, semi-arid drylands are generally characterized by strong rainfall and fire seasonality and dominating land cover types from driest to more humid regions are: grasslands, savannas, woody savannas and forest. In northern America and Eurasia, semi-arid drylands also face distinct wet-dry periods, and often also hot summers and cold winters. Here, dominating land cover in the driest areas is grassland, while more humid regions have often been converted to cropland.

The distribution of trends in vegetation indices differs between humidity classes and land cover classes (Fig. 8). The median trend in NDVI is around zero for semi-arid drylands as a whole, showing positive trends over savannas and croplands and negative median trends for other land cover classes. VOD shows positive median trends for all land cover classes except forest (see Fig. 8a and d). In most semi-arid areas where savanna grasslands dominate resources are available to support forests, but they are suppressed by frequent fire (Bond and Keeley, 2005), which is thought to be the next most important driver of vegetation variation in savannas after precipitation (Sankaran et al., 2005).

Although northern and southern African semi-arid drylands experience similar increasing trends in precipitation (Fig. 10a), the changes in the vegetation indices are very different. In southern Africa (i.e., south of 5°S), minimum annual NDVI values are declining, resulting in overall decreasing trends in NDVI, while VOD trends are increasing; likely caused by an increase in woody component. Northern African savannas (in contrast with the grasslands in adjacent arid drylands), show increasing trends in NDVI largely due to increased recurrent vegetation, along with increasing trends (in most regions) for VOD; interpreted as an increase in the herbaceous component or increase in total AGB. The increasing trend in the north African grasslands and savannas is widely discussed in literature and has been explained as a result of recovery after drought (1983-1985 being the driest years; Anyamba and Tucker, 2005) and improved land management (e.g., irrigation, and soil and water conservation; Herrmann et al., 2005). Observed increases in wet season length in semi-arid parts of the region likely cause increasing trends, especially in NDVI (de Jong et al., 2011). Some of the strongest trends in both persistent and recurrent NDVI components occur in semi-arid areas with large annual burned area (compare Fig. 9a and b with 10d). Northern African savannas, with recent declines in annual burned area (Fig. 10b), showed stable minimum NDVI values (Fig. 9a) with an increasing recurrent vegetation component (Fig. 9b). Widespread grazing (Fig. 10c), with associated fire suppression may explain decreasing annual burned area in northern Africa between 2001 and 2011 (Fig. 10b; Archibald et al., 2010). Southern African regions, with recent increases in annual burned area, showed declining minimum NDVI values with regrowth in the wet season. There may have been an increase in Net Primary Production (NPP), with associated increases in fire activity (Bowman et al., 2009), which would explain the increase in recurrent NDVI. Human land use practice is also thought to be an important driver of annual burned area (Archibald et al., 2009). The effect of fire on vegetation indices is most profound in African and Australian savannas and woody savannas, where annual burned area typically ranges from 20 to 80% (Fig. 10d). In areas of high NPP, fire limits vegetation growth in the dry seasons, while in areas of low NPP fire is limited by NPP of the preceding season(s). Given the high percentage of area burnt each year in many African savannas and woody savannas (Fig. 11), it seems feasible that changing fire regimes rather than changes in the persistent or recurrent vegetation components

per se cause the observed trend in NDVI.

Outside the African savannas and woody savannas, the residual trends in NDVI are not easily attributed to changes in annual burned area, at least not using the data available to us. While even in the less fire prone regions, fire might play a crucial role in species competition, the direct effect of the smaller relative area of fire scars on the vegetation indices would be limited. Other drivers also affect vegetation dynamics, with the impact of fire on vegetation dynamics in other land cover types being less pronounced than in savannas (Fig. 11). Persistent NDVI might also be affected by grazing; while any given area might support livestock during most times, the highest pressure on vegetation occurs during longer dry seasons. The negative trends in both persistent NDVI and VOD over the South American dry forests might be caused by deforestation, that is reducing the persistent/woody vegetation component (Grau et al., 2005).

Trends in VOD occurred in areas of frequent fire, but no coherent spatial pattern was apparent (compare Fig. 7f, 9c and 9d with 10b and 10d). Although fire suppresses woody encroachment, dryland fires generally have a relatively low temperature and flame height and therefore do not necessarily affect established woody vegetation much (Bond and Keeley, 2005). Woody vegetation appears to increase in the southern African savannas despite increased burning (Fig. 10b and 12). This may partly be explained by increasing precipitation (Fig. 7; Sankaran et al., 2005), CO_2 fertilization (Buitenwerf et al., 2011; Higgins and Scheiter, 2012) and/or grazing by non domesticated herbivores. A clear increasing NDVI and VOD trend was found for croplands and adjacent grasslands in the USA. Woody encroachment in US grasslands has been widely reported (see Archer et al., 2001, and the references therein) and although there is no straightforward single driver, grazing is understood to play an important role (Van Auken, 2000; Briggs et al., 2005). Increasing agricultural activity might however also play an important role driving those trends (Neigh et al., 2008).

The strongest positive median NDVI and VOD trends were found in agricultural areas (Fig. 8). Increases of both indices over the world's agricultural regions are explained by advances in

agricultural practice including mechanization, irrigation and fertilization (Liu et al., 2012). In India, Pakistan, Bangladesh, China, Ukraine, southwestern Russia, several European countries, the USA, and a number of other countries, substantial areas of agricultural land are irrigated (Wada et al., 2010). Evidence that increasing trends in NDVI are caused by irrigation and fertilization has been documented for India (Jeyaseelan et al., 2007) and the North China Plain (Piao et al., 2003), while Liu et al. (2012) showed that positive VOD trends in southern Russia, China, India and the US are probably also the result of increased agricultural production. Negative trends in minimum NDVI values over Russian croplands (causing an overall negative trend in NDVI) are caused by changing wintertime NDVI values and might be related to changing snow cover, and/or an increase in winter time bare land (Fig. 9a). In drylands at higher latitudes both water and temperature are factors limiting vegetation growth (Nemani et al., 2003), and global changes in temperature can therefore also explain some of the vegetation trends (Tucker et al., 2001).

7 Conclusions

A recently developed passive microwave vegetation dataset (VOD) and a widely used reflective based vegetation dataset (NDVI) were combined to study the long-term (1988-2008) vegetation changes over the world's drylands. We could draw the following conclusions:

i The two data sets provide complementary information on vegetation dynamics; NDVI being most responsive to canopy cover and greenness, and VOD to vegetation above-ground biomass.

ii NDVI was more sensitive to herbaceous vegetation changes and short-term precipitation variations. VOD, on the other hand, was more sensitive to changes in woody vegetation and longer term precipitation variations.

iii Although precipitation is an important driver for dryland vegetation dynamics, precipitation variations could not explain all of the observed trends in vegetation indices.

iv Comparing trends in NDVI and VOD helps to interpret and sometimes attribute large-scale vegetation changes. For the world's drylands an overall NDVI decrease and VOD increase were observed. Combined, these results provide evidence for increases in woody biomass in many drylands.

v Co-relationship between NDVI and VOD provides evidence of widespread woody vegetation encroachment at the expense of the herbaceous vegetation component in arid regions (humidity <0.3), and arid shrublands in particular. Spatial distribution of trends suggests that a global driver (e.g., CO_2 fertilization) is causing a change in relative performance of woody vegetation compared to herbaceous vegetation.

vi Globally, remote sensing evidence for woody thickening and encroachment is also found for some semi-arid drylands, but regional trends vary widely. It is interpreted that local rather than global drivers are responsible for most of the observed residual trends in these areas. Limited observations of monthly burned area suggests that after precipitation, changing fire regimes are an important driver of vegetation change in semi-arid drylands, especially in savannas.

vii In regions of frequent fire, both NDVI and VOD minimum values seem to be strongly affected by annual burned area. This should be taken into consideration when annual minima are used to calculate the persistent and recurrent vegetation components and when these are used to infer the dynamics of evergreen and seasonal or woody and non-woody vegetation components, respectively.

viii Large changes in vegetation density were observed in agricultural dryland regions, where advances in agricultural practices caused increasing trends in both vegetation indices.

In summary, we demonstrated that using two complementary vegetation indices provide new insights into the dynamics of different vegetation components in global drylands. While it remains challenging to attribute dryland vegetation dynamics to any individual driver, a linear precipitation response model showed that many changes cannot be attributed to precipitation alone. Global data on fire regimes and grazing enabled a first assessment of the likely relative

importance of these drivers on global vegetation change. Future improvements and extensions to time series of fire characteristics, grazing and land use change are likely to further improve understanding of global vegetation changes and its drivers.

Acknowledgements. The authors thank Jorge E. Pinzon and C. Jim Tucker (both with NASA, Biospheric Science Branch, Goddard Space Flight Center, Maryland, USA) for providing access to the NDVI GIMMS3g dataset (1981-2010).

References

Adamoli, J., Sennhauser, E., Acero, J. M., and Rescia, A.: Stress and disturbance: vegetation dynamics in the dry Chaco region of Argentina, Journal of Biogeography, 17, 491–500, 1990.

Allen, C. D., Macalady, A. K., Chenchouni, H., Bachelet, D., McDowell, N., Vennetier, M., Kitzberger, T., Rigling, A., Breshears, D. D., Hogg, E. H., Gonzalez, P., Fensham, R., Zhang, Z., Castro, J., Demidova, N., Lim, J. H., Allard, G., Running, S. W., Semerci, A., and Cobb, N.: A global overview of drought and heat-induced tree mortality reveals emerging climate change risks for forests, Forest Ecology and Management, 259, 660–684, 2010.

Anyamba, A. and Tucker, C. J.: Analysis of Sahelian vegetation dynamics using NOAA-AVHRR NDVI data from 1981-2003, Journal of Arid Environments, 63, 596–614, 2005.

Archer, S., Schimel, D. S., and Holland, E. A.: Mechanisms of shrubland expansion: land use, climate or CO_2?, Climatic Change, 29, 91–99, 1995.

Archer, S., Boutton, T. W., and Hibbard, K. A.: Trees in grasslands: biogeochemical consequences of woody plant expansion. In: Global Biogeochemical Cycles in the Climate System, pp. 115–138, Academic Press: San Diego, 2001.

Archibald, S. and Scholes, R. J.: Leaf green-up in a semi-arid African savanna-separating tree and grass responses to environmental cues, Journal of Vegetation Science, 18, 583–594, 2007.

Archibald, S., Roy, D. P., van Wilgen, B. W., and Scholes, R. J.: What limits fire? An examination of drivers of burnt area in Southern Africa, Global Change Biology, 15, 613–630, 2009.

Archibald, S., Scholes, R. J., Roy, D. P., Roberts, G., and Boschetti, L.: Southern African fire regimes as revealed by remote sensing, International Journal of Wildland Fire, 19, 861–878, 2010.

Asner, G. P.: Biophysical and biochemical sources of variability in canopy reflectance, Remote Sensing of Environment, 64, 234–253, 1998.

Asner, G. P., Borghi, C. E., and Ojeda, R. A.: Desertification in central Argentina: changes in ecosystem carbon and nitrogen from imaging spectroscopy, Ecological Applications, 13, 629–648, 2003.

Asner, G. P., Elmore, A. J., Olander, L. P., Martin, R. E., and Harris, A. T.: Grazing systems, ecosystem responses, and global change, Annual Review of Environment and Resources, 29, 261–299, 2004.

Asrar, G., Fuchs, M., Kanemasu, E. T., and Hatfield, J. L.: Estimating absorbed photosynthetic radiation and leaf area index from spectral reflectance in wheat, Agronomy Journal, 76, 300, 1984.

Bai, Z. G., Dent, D. L., Olsson, L., and Schaepman, M. E.: Proxy global assessment of land degradation, Soil Use and Management, 24, 223–234, 2008.

Beck, H. E., McVicar, T. R., van Dijk, A. I. J. M., Schellekens, J., de Jeu, R. A. M., and Bruijnzeel, L. A.: Global evaluation of four AVHRR-NDVI data sets: Intercomparison and assessment against Landsat imagery, Remote Sensing of Environment, 115, 2547–2563, 2011.

Bond, W. J. and Keeley, J. E.: Fire as a global 'herbivore': the ecology and evolution of flammable ecosystems, Trends in Ecology & Evolution, 20, 387–394, 2005.

Bond, W. J. and Midgley, G. F.: Carbon dioxide and the uneasy interactions of trees and savannah grasses, Philosophical Transactions of the Royal Society B: Biological Sciences, 367, 601–612, 2012.

Bond, W. J., Midgley, G. F., and Woodward, F. I.: The importance of low atmospheric CO_2 and fire in promoting the spread of grasslands and savannas, Global Change Biology, 9, 973–982, 2003.

Bond, W. J., Woodward, F. I., and Midgley, G. F.: The global distribution of ecosystems in a world without fire, New Phytologist, 165, 525–538, 2005.

Bowman, D. M. J. S., Balch, J. K., Artaxo, P., Bond, W. J., Carlson, J. M., Cochrane, M. A., D'Antonio, C. M., DeFries, R. S., Doyle, J. C., Harrison, S. P., Johnston, F. H., Keeley, J. E., Krawchuk, M. A., Kull, C. A., Marston, J. B., Moritz, M. A., Prentice, I. C., Roos, C. I., Scott, A. C., Swetnam, T. W., Werf, v. d. G. R., and Pyne, S. J.: Fire in the Earth system, Science, 324, 481–484, 2009.

Breshears, D. D.: The grassland-forest continuum: trends in ecosystem properties for woody plant mosaics?, Frontiers in Ecology and the Environment, 4, 96–104, 2006.

Briggs, J. M., Knapp, A. K., Blair, J. M., Heisler, J. L., Hoch, G. A., Lett, M. S., and McCarron, J. K.: An ecosystem in transition: causes and consequences of the conversion of mesic grassland to shrubland, BioScience, 55, 243–254, 2005.

Brooks, M. L., D'Antonio, C. M., Richardson, D. M., Grace, J. B., Keeley, J. E., DiTomaso, J. M., Hobbs, R. J., Pellant, M., and Pyke, D.: Effects of invasive alien plants on fire regimes, BioScience, 54, 677–688, 2004.

Brown, M. E., Pinzón, J. E., Didan, K., Morisette, J. T., and Tucker, C. J.: Evaluation of the consistency of long-term NDVI time series derived from AVHRR, SPOT-Vegetation, SeaWiFS, MODIS, and Landsat ETM+ sensors, IEEE Transactions on Geoscience and Remote Sensing, 44, 1787–1793, 2006.

Buitenwerf, R., Bond, W. J., Stevens, N., and Trollope, W. S. W.: Increased tree densities in South African savannas:>50 years of data suggests CO_2 as a driver, Global Change Biology, 18, 675–684, 2011.

Carlson, T. N. and Ripley, D. A.: On the relation between NDVI, fractional vegetation cover, and leaf area index, Remote Sensing of Environment, 62, 241–252, 1997.

de Jeu, R. A. M.: Retrieval of Land Surface Parameters using Passive Microwave Remote Sensing, Ph.D. thesis, VU University, Amsterdam, 2003.

de Jong, R., de Bruin, S., de Wit, A., Schaepman, M. E., and Dent, D. L.: Analysis of monotonic greening and browning trends from global NDVI time-series, Remote Sensing of Environment, 115, 692–702, 2011.

Díaz-Delgado, R., Lloret, F., and Pons, X.: Influence of fire severity on plant regeneration by means of remote sensing imagery, International Journal of Remote Sensing, 24, 1751–1763, 2003.

Donohue, R. J., McVicar, T. R., and Roderick, M. L.: Climate-related trends in Australian vegetation cover as inferred from satellite observations, 1981–2006, Global Change Biology, 15, 1025–1039, 2009.

Dore, M. H. I.: Climate change and changes in global precipitation patterns: What do we know?, Environment International, 31, 1167–1181, 2005.

Drake, B. G., Gonzàlez-Meler, M. A., and Long, S. P.: More efficient plants: a consequence of rising atmospheric CO_2?, Annual Review of Plant Biology, 48, 609–639, 1997.

Evans, J. and Geerken, R.: Discrimination between climate and human-induced dryland degradation, Journal of Arid Environments, 57, 535–554, 2004.

Farquhar, G. D.: Carbon dioxide and vegetation, Science, 278, 1411–1411, 1997.

Fensham, R. J., Fairfax, R. J., and Archer, S. R.: Rainfall, land use and woody vegetation cover change in semi-arid Australian savanna, Journal of Ecology, 93, 596–606, 2005.

Fensholt, R., Langanke, T., Rasmussen, K., Reenberg, A., Prince, S. D., Tucker, C. J., Scholes, R. J., Bao Le, Q., Bondeau, A., Eastman, R., Epstein, H., Gaughan, A. E., Hellden, U., Mbow, C., Olsson, L., Paruelo, J., Schweitzer, C., Seaquist, J., and Wessels, K.: Greenness in semi-arid areas across the globe 1981-2007 - an Earth Observing Satellite based analysis of trends and drivers, Remote Sensing of Environment, 121, 144–158, 2012.

Flannigan, M. D., Krawchuk, M. A., De Groot, W. J., Wotton, B. M., and Gowman, L. M.: Implications of changing climate for global wildland fire, International Journal of Wildland Fire, 18, 483–507, 2009.

Giglio, L., Loboda, T., Roy, D. P., Quayle, B., and Justice, C. O.: An active-fire based burned area mapping algorithm for the MODIS sensor, Remote Sensing of Environment, 113, 408–420, 2009.

Gouweleeuw, B. T., van Dijk, A. I. J. M., Guerschman, J. P., Dyce, P., de Jeu, R. A. M., and Owe, M.: Assimilation of space-based passive microwave soil moisture retrievals and the correction for a dynamic open water fraction, Hydrol. Earth Syst. Sci. Discuss, 9, 1013–1039, 2012.

Grau, H. R., Gasparri, N. I., and Aide, T. M.: Agriculture expansion and deforestation in seasonally dry forests of north-west Argentina, Environmental Conservation, 32, 140–148, 2005.

Hansen, M. C., DeFries, R. S., Townshend, J. R. G., and Sohlberg, R.: Global land cover classification at 1 km spatial resolution using a classification tree approach, International Journal of Remote Sensing, 21, 1331–1364, 2000.

Heisler, J. L., Briggs, J. M., and Knapp, A. K.: Long-term patterns of shrub expansion in a C4-dominated grassland: fire frequency and the dynamics of shrub cover and abundance, American Journal of Botany, 90, 423–428, 2003.

Herrmann, S. M., Anyamba, A., and Tucker, C. J.: Recent trends in vegetation dynamics in the African Sahel and their relationship to climate, Global Environmental Change Part A, 15, 394–404, 2005.

Higgins, S. I. and Scheiter, S.: Atmospheric CO_2 forces abrupt vegetation shifts locally, but not globally, Nature, 488, 209–212, 2012.

Hijmans, R. J., Cameron, S. E., Parra, J. L., Jones, P. G., and Jarvis, A.: Very high resolution interpolated climate surfaces for global land areas, International Journal of Climatology, 25, 1965–1978, 2005.

House, J. I., Archer, S., Breshears, D. D., and Scholes, R. J.: Conundrums in mixed woody–herbaceous plant systems, Journal of Biogeography, 30, 1763–1777, 2003.

Huete, A. R., Jackson, R. D., and Post, D. F.: Spectral response of a plant canopy with different soil backgrounds, Remote Sensing of Environment, 17, 37–53, 1985.

Jackson, T. J., Schmugge, T. J., and Wang, J. R.: Passive microwave sensing of soil moisture under vegetation canopies, Water Resources Research, 18, 1137–1142, 1982.

Jahnke, H. E.: Livestock production systems and livestock development in tropical Africa, Kieler Wissenschaftsverlag Vauk: Kiel, available from: http://pdf.usaid.gov/pdf_docs/pnaan484.pdf, 1982.

Jeyaseelan, A. T., Roy, P. S., and Young, S. S.: Persistent changes in NDVI between 1982 and 2003 over India using AVHRR GIMMS (Global Inventory Modeling and Mapping Studies) data, International Journal of Remote Sensing, 28, 4927–4946, 2007.

Jones, M. O., Jones, L. A., Kimball, J. S., and McDonald, K. C.: Satellite passive microwave remote sensing for monitoring global land surface phenology, Remote Sensing of Environment, 115, 1102–1114, 2011.

Jones, M. O., Kimball, J. S., Jones, L. A., and McDonald, K. C.: Satellite passive microwave detection of North America start of season, Remote Sensing of Environment, 123, 324–333, 2012.

Jones, P. and Harris, I.: CRU Time Series (TS) high resolution gridded datasets, university of East Anglia Research Unit (CRU) NCAS British Atmospheric Data Centre, available from http://badc.nerc.ac.uk/view/badc.nerc.ac.uk__ATOM__dataent_1256223773328276, 2008.

Kaufman, Y. J., Justice, C. O., Flynn, L. P., Kendall, J. D., Prins, E. M., Giglio, L., Ward, D. E., Menzel, W. P., and Setzer, A. W.: Potential global fire monitoring from EOS-MODIS, Journal of Geophysical Research, 103, 32 215–32, 1998.

Kirdiashev, K. P., Chukhlantsev, A. A., and Shutko, A. M.: Microwave radiation of the Earth's surface in the presence of vegetation cover, Radio Engineering and Electronic Physics, 24, 37–44, 1979.

Lehmann, C. E. R., Archibald, S. A., Hoffmann, W. A., and Bond, W. J.: Deciphering the distribution of the savanna biome, New Phytologist, 191, 197–209, 2011.

Liu, Y. Y., de Jeu, R. A. M., van Dijk, A. I. J. M., and Owe, M.: TRMM-TMI satellite observed soil moisture and vegetation density (1998–2005) show strong connection with El Niño in eastern Australia, Geophysical Research Letters, 34, L15 401, doi:10.1029/2007GL030 311, 2007.

Liu, Y. Y., de Jeu, R. A. M., McCabe, M. F., Evans, J. P., and van Dijk, A. I. J. M.: Global long-term passive microwave satellite-based retrievals of vegetation optical depth, Geophysical Research Letters, 38, L18 402, doi:10.1029/2011GL048 684, 2011a.

Liu, Y. Y., Parinussa, R. M., Dorigo, W. A., de Jeu, R. A. M., Wagner, W., Van Dijk, A. I. J. M., McCabe, M. F., and Evans, J. P.: Developing an improved soil moisture dataset by blending passive and active microwave satellite-based retrievals, Hydrology and Earth System Sciences, 15, 425, 2011b.

Liu, Y. Y., Dijk, A. I. J. M., McCabe, M. F., Evans, J. P., and de Jeu, R. A. M.: Global vegetation biomass change (1988–2008) and attribution to environmental and human drivers, Global Ecology and Biogeography, doi:10.1111/geb.12024, 2012.

Liu, Y. Y., Evans, J. P., McCabe, M. F., de Jeu, R. A. M., van Dijk, A. I. J. M., Dolman, A. J., and Saizen, I.: Changing Climate and Overgrazing Are Decimating Mongolian Steppes, PloS one, 8, e57 599, 2013.

Lu, H., Raupach, M. R., McVicar, T. R., and Barrett, D. J.: Decomposition of vegetation cover into woody and herbaceous components using AVHRR NDVI time series, Remote Sensing of Environment, 86, 1–18, 2003.

McMahon, S. M., Parker, G. G., and Miller, D. R.: Evidence for a recent increase in forest growth, Proceedings of the National Academy of Sciences of the USA, 107, 3611–3615, 2010.

McVicar, T. R. and Jupp, D. L. B.: The current and potential operational uses of remote sensing to aid decisions on drought exceptional circumstances in Australia: a review, Agricultural Systems, 57, 399–468, 1998.

McVicar, T. R., Roderick, M. L., Donohue, R. J., Li, L. T., Van Niel, T. G., Thomas, A., Grieser, J., Jhajharia, D., Himri, Y., Mahowald, N. M., Mescherskaya, A. V., Kruger, A. C., Rehman, S., Dinpashoh, Y., and Rehman, S.: Global review and synthesis of trends in observed terrestrial near-surface wind speeds: Implications for evaporation, Journal of Hydrology, 416–417, 182–205, 2012.

Meesters, A. G. C. A., De Jeu, R. A. M., and Owe, M.: Analytical derivation of the vegetation optical depth from the microwave polarization difference index, IEEE, Geoscience and Remote Sensing Letters, 2, 121–123, 2005.

Monsi, M. and Saeki, T.: On the factor light in plant communities and its importance for matter production, Annals of Botany, 95, 549–567, 2005.

NASA: Land Processes Distribute Active Archive Center, MODIS/Terra+Aqua Land Cover Type Yearly L3 Global 0.05Deg CMG V005, U.S. Geological Survey, available from: ftp://e4ftl01.cr.usgs.gov/MOTA/MCD12C1.005/2008.01.01/, 2008.

Neigh, C. S., Tucker, C. J., and Townshend, J. R.: North American vegetation dynamics observed with multi-resolution satellite data, Remote Sensing of Environment, 112, 1749–1772, 2008.

Nemani, R. R., Keeling, C. D., Hashimoto, H., Jolly, W. M., Piper, S. C., Tucker, C. J., Myneni, R. B., and Running, S. W.: Climate-driven increases in global terrestrial net primary production from 1982 to 1999, Science, 300, 1560–1563, 2003.

Nicholson, S. E. and Farrar, T. J.: The influence of soil type on the relationships between NDVI, rainfall, and soil moisture in semiarid Botswana. I. NDVI response to rainfall, Remote Sensing of Environment, 50, 107–120, 1994.

Nicholson, S. E., Davenport, M. L., and Malo, A. R.: A comparison of the vegetation response to rainfall in the Sahel and East Africa, using normalized difference vegetation index from NOAA AVHRR, Climatic Change, 17, 209–241, 1990.

Northup, B. K., Zitzer, S. F., Archer, S., McMurtry, C. R., and Boutton, T. W.: Above-ground biomass and carbon and nitrogen content of woody species in a subtropical thornscrub parkland, Journal of Arid Environments, 62, 23–43, 2005.

Ovington, J. D., Haitkamp, D., and Lawrence, D. B.: Plant biomass and productivity of prairie, savanna, oakwood, and maize field ecosystems in central Minnesota, Ecology, 44, 52–63, 1963.

Owe, M., de Jeu, R. A. M., and Walker, J.: A methodology for surface soil moisture and vegetation optical depth retrieval using the microwave polarization difference index, IEEE Transactions on Geoscience and Remote Sensing, 39, 1643–1654, 2001.

Owe, M., de Jeu, R. A. M., and Holmes, T. R. H.: Multi-Sensor Historical Climatology of Satellite-Derived Global Land Surface Moisture, Journal of Geophysical Research, 113, F01 002, doi:1029/2007JF000 769, 2008.

Pettorelli, N., Vik, J. O., Mysterud, A., Gaillard, J. M., Tucker, C. J., and Stenseth, N. C.: Using the satellite-derived NDVI to assess ecological responses to environmental change, Trends in Ecology & Evolution, 20, 503–510, 2005.

Piao, S. L., Fang, J. Y., Zhou, L. M., Guo, Q. H., Henderson, M., Ji, W., Li, Y., and Tao, S.: Interannual variations of monthly and seasonal normalized difference vegetation index (NDVI) in China from 1982 to 1999, Journal of Geophysical Research, 108, 4401, doi:10.1029/2002JD002 848, 2003.

Reich, P. B., Walters, M. B., and Ellsworth, D. S.: From tropics to tundra: global convergence in plant functioning, Proceedings of the National Academy of Sciences of the USA, 94, 13 730–13 734, 1997.

Reich, P. B., Wright, I. J., Cavender-Bares, J., Craine, J. M., Oleksyn, J., Westoby, M., and Walters, M. B.: The evolution of plant functional variation: traits, spectra, and strategies, International Journal of Plant Sciences, 164, S143–S164, 2003.

Robinson, T. P., Franceschini, G., and Wint, W.: The Food and Agriculture Organization's gridded livestock of the world, Veterinaria Italiana, 43, 745–751, 2007.

Roderick, M. L., Berry, S. L., Saunders, A. R., and Noble, I. R.: On the relationship between the composition, morphology and function of leaves, Functional Ecology, 13, 696–710, 1999a.

Roderick, M. L., Noble, I. R., and Cridland, S. W.: Estimating woody and herbaceous vegetation cover from time series satellite observations, Global Ecology and Biogeography, 8, 501–508, 1999b.

Roderick, M. L., Berry, S. L., and Noble, I. R.: A framework for understanding the relationship between environment and vegetation based on the surface area to volume ratio of leaves, Functional Ecology, 14, 423–437, 2000.

Rossatto, D. R., da Silveira Lobo Sternberg, L., and Franco, A. C.: The partitioning of water uptake between growth forms in a Neotropical savanna: do herbs exploit a third water source niche?, Plant Biology, pp. doi:10.1111/j.1438–8677.2012.00 618.x, 2012.

Rouse, J. W., Haas, R. H., Schell, J. A., Deering, D. W., and Harlan, J. C.: Monitoring the vernal advancement of retrogradation of natural vegetation, NASA/GSFC, Tech. rep., Greenbeld, MD, available from: http://ntrs.nasa.gov/archive/nasa/casi.ntrs.nasa.gov/19740004927_1974004927.pdf, 1974.

Sankaran, M., Hanan, N. P., Scholes, R. J., Ratnam, J., Augustine, D. J., Cade, B. S., Gignoux, J., Higgins, S. I., Le Roux, X., Ludwig, F., Ardo, J., Banyikwa, F., Bronn, A., Bucini, G., Caylor, K. K., Coughenour, M. B., Diouf, A., Ekaya, W., Feral, C. J., February, E. C., Frost, P. H., Hiernayx, P., Hrabar, H., Metzger, K. L., Prins, H. H. T., Ringrose, S., Sea, W., Tews, J., Worden, J., and Zambatis, N.: Determinants of woody cover in African savannas, Nature, 438, 846–849, 2005.

Sankey, J. B., Ravi, S., Wallace, C. S. A., Webb, R. H., and Huxman, T. E.: Quantifying soil surface change in degraded drylands: Shrub encroachment and effects of fire and vegetation removal in a desert grassland, Journal of Geophysical Research, 117, G02 025, doi:10.1029/2012JG002 002, 2012.

Sen, P. K.: Estimates of the regression coefficient based on Kendall's tau, Journal of the American Statistical Association, 63, 1379–1389, 1968.

Shi, J., Jackson, T., Tao, J., Du, J., Bindlish, R., Lu, L., and Chen, K. S.: Microwave vegetation indices for short vegetation covers from satellite passive microwave sensor AMSR-E, Remote Sensing of Environment, 112, 4285–4300, 2008.

Sternberg, M. and Shoshany, M.: Aboveground biomass allocation and water content relationships in Mediterranean trees and shrubs in two climatological regions in Israel, Plant Ecology, 157, 173–181, 2001.

Theil, H.: A rank-invariant method of linear and polynomial regression analysis, Proceedings of Koninklijke Nederlandse Akademie van Wetenschappen, 53, 386–392,521–525,1397–1412, 1950.

Tietjen, B., Jeltsch, F., Zehe, E., Classen, N., Groengroeft, A., Schiffers, K., and Oldeland, J.: Effects of climate change on the coupled dynamics of water and vegetation in drylands, Ecohydrology, 3, 226–237, 2010.

Tottrup, C. and Rasmussen, M. S.: Mapping long-term changes in savannah crop productivity in Senegal through trend analysis of time series of remote sensing data, Agriculture, Ecosystems & Environment, 103, 545–560, 2004.

Tucker, C. J.: Red and photographic infrared linear combinations for monitoring vegetation, Remote Sensing of Environment, 8, 127–150, 1979.

Tucker, C. J., Vanpraet, C. L., Sharman, M. J., and Van Ittersum, G.: Satellite remote sensing of total herbaceous biomass production in the Senegalese Sahel: 1980-1984, Remote Sensing of Environment, 17, 233–249, 1985.

Tucker, C. J., Slayback, D. A., Pinzon, J. E., Los, S. O., Myneni, R. B., and Taylor, M. G.: Higher northern latitude normalized difference vegetation index and growing season trends from 1982 to 1999, International Journal of Biometeorology, 45, 184–190, 2001.

Tucker, C. J., Pinzon, J. E., Brown, M. E., Slayback, D. A., Pak, E. W., Mahoney, R., Vermote, E. F., and El Saleous, N.: An extended AVHRR 8-km NDVI dataset compatible with MODIS and SPOT vegetation NDVI data, International Journal of Remote Sensing, 26, 4485–4498, 2005.

Van Auken, O. W.: Shrub invasions of North American semiarid grasslands, Annual Review of Ecology and Systematics, 31, 197–215, 2000.

Vegten, J. A.: Thornbush invasion in a savanna ecosystem in eastern Botswana, Plant Ecology, 56, 3–7, 1984.

Wada, Y., van Beek, L. P. H., van Kempen, C. M., Reckman, J. W. T. M., Vasak, S., and Bierkens, M. F. P.: Global depletion of groundwater resources, Geophysical Research Letters, 37, L20 402, doi:10.1029/2010GL044 571, 2010.

Wang, Q., Adiku, S., Tenhunen, J., and Granier, A.: On the relationship of NDVI with leaf area index in a deciduous forest site, Remote Sensing of Environment, 94, 244–255, 2005.

Wessels, K. J., Prince, S. D., Malherbe, J., Small, J., Frost, P. E., and VanZyl, D.: Can human-induced land degradation be distinguished from the effects of rainfall variability? A case study in South Africa, Journal of Arid Environments, 68, 271–297, 2007.

Wigneron, J. P., Kerr, Y., Chanzy, A., and Jin, Y. Q.: Inversion of surface parameters from passive microwave measurements over a soybean field, Remote Sensing of Environment, 46, 61–72, 1993.

Zomer, R. J., Trabucco, A., Bossio, D. A., and Verchot, L. V.: Climate change mitigation: A spatial analysis of global land suitability for clean development mechanism afforestation and reforestation, Agriculture, Ecosystems & Environment, 126, 67–80, 2008.

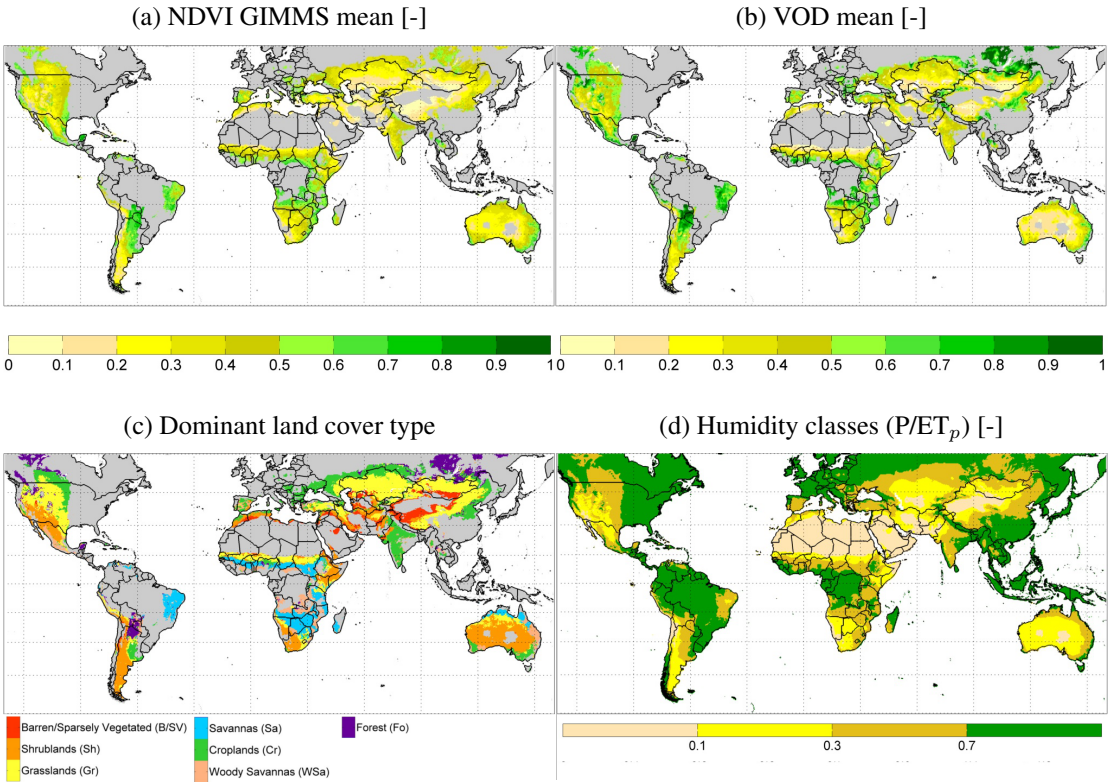

Fig. 1. Mean values of vegetation indices (1988-2008) and characterization of ecosystems in terms of land cover and humidity. Part (a) Mean NDVI; part (b) mean VOD; part (c) MODIS dominant land cover type, herein referred to as land cover; and part (d) humidity classes, based on 50-year average (1950-2000) precipitation (P) data (Hijmans et al., 2005) and potential evaporation (ET$_p$) data (Zomer et al., 2008). All maps in this paper (except for Fig. 3d) are projected in the Miller Cylindrical projection (60°N-60°S, 130°W-160°E). Terrestrial areas that are not drylands (as defined in this paper) are masked grey in all figures and are excluded from analysis, and oceans are masked (white) in all figures.

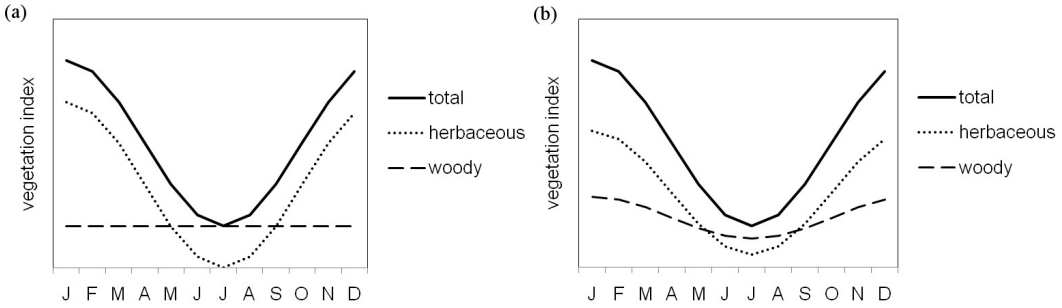

Fig. 2. Hypothetical models of the relative contribution of woody and herbaceous vegetation to observed values of vegetation indices. Part (a) is the most parsimonious model, used in this paper and part (b) includes seasonal variation of the woody component.

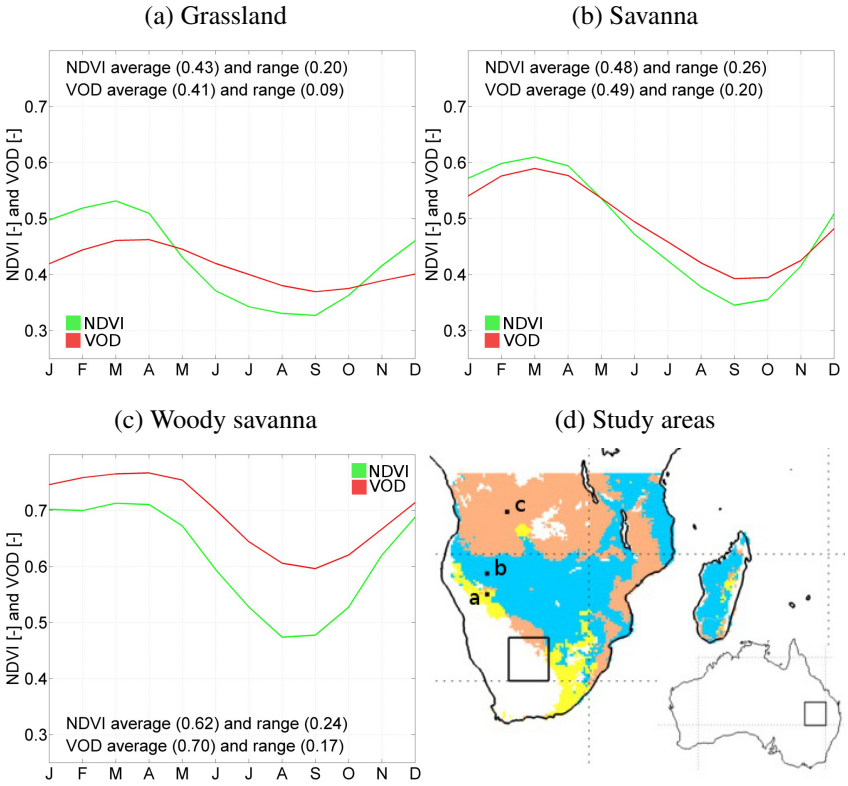

Fig. 3. Long-term (1988-2008) average monthly NDVI and VOD signals for three common land cover classes of southern Africa (5-35°S,10-50°E) and a map of study areas. Part (a) is grassland (733 0.25° resolution grid cells); (b) savanna (4041 0.25° resolution grid cells); and (c) woody savanna (3826 0.25° resolution grid cells). The annual average and range of both vegetation indices are reported on each sub-plot. Part (d) shows an overview of the study areas used in figures 6, 3 and 11. Australia is shown at half the scale of southern Africa. The three regions, based on land cover, used in Fig. 3a, b and c are shown in yellow (grassland), blue (savanna) and pink (woody savanna).

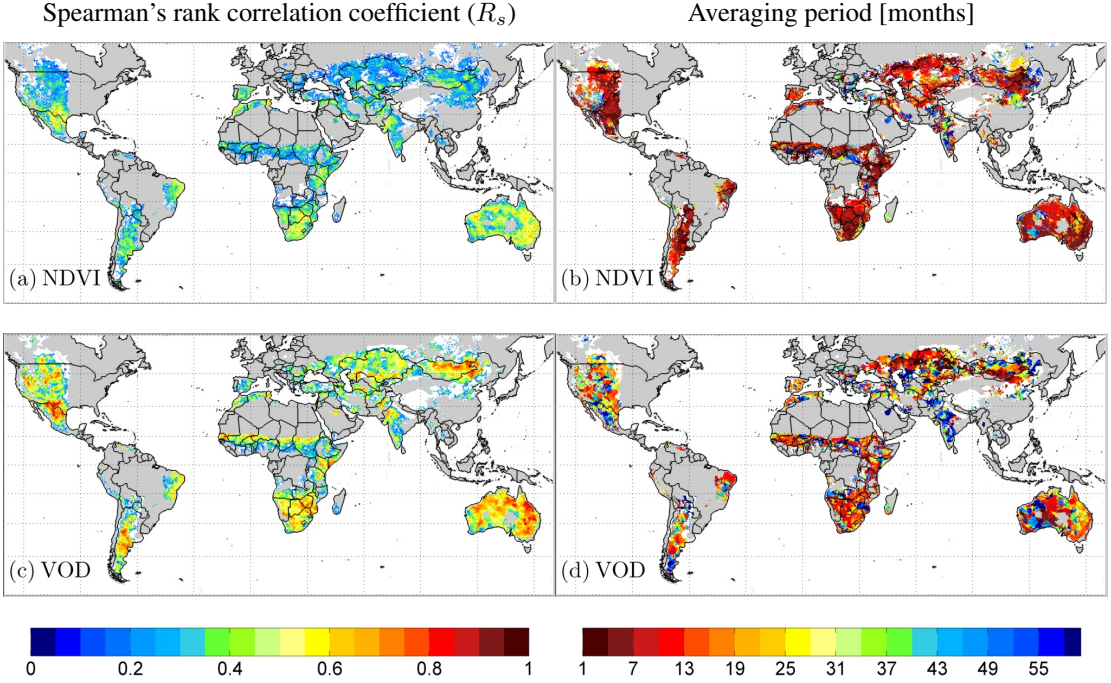

Fig. 4. Spearman's rank correlation coefficient (R_s) and averaging periods for the two vegetation indices. For the NDVI part (a) is the R_s between API and the NDVI anomaly and part (b) is the averaging period for antecedent precipitation that leads to the highest R_s between PRM and the vegetation anomalies (denoted as T in the methods). Parts (c) and (d) are as (a) and (b) except for the VOD. Grid cells without significant correlation (p <0.05), with over 60 % missing values, or with a negative correlation coefficients are masked (white).

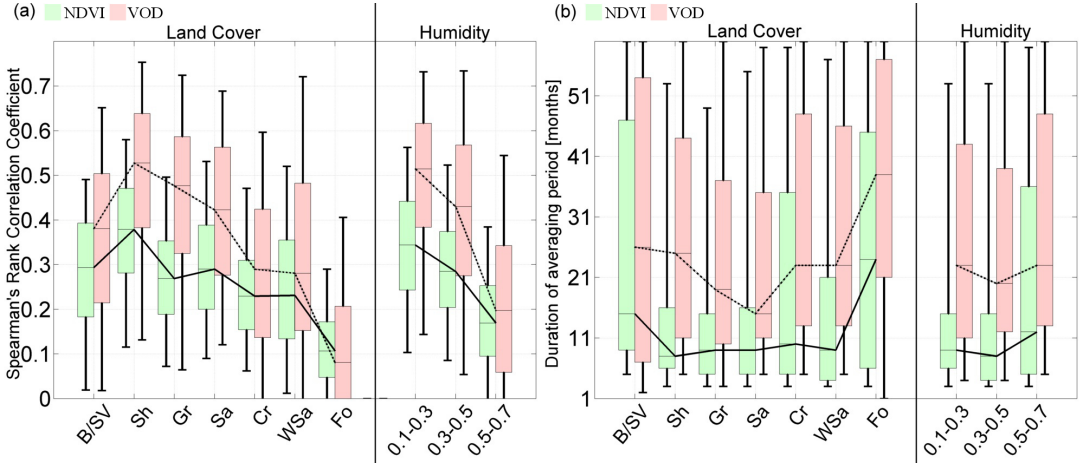

Fig. 5. Box plots showing the distribution of R_s and averaging periods for the two vegetation indices. Part (a) distribution of R_s between observed vegetation anomalies and API for NDVI and VOD, stratified by: (left) land cover classes and (right) humidity classes; and part (b) the distribution of the duration of averaging period for antecedent precipitation that leads to strongest correlation between the PRM and observed vegetation anomalies, stratified by: (left) land cover classes and (right) humidity classes. Solid lines indicate the NDVI medians and dash-dot lines the VOD medians. The maximum and minimum extents of the colored boxes indicate 25th and 75th percentiles and whiskers represent the 5th and 95th percentiles. Grid cells with over 60 % missing values are not included in this figure, and grid cells without significant correlation ($p > 0.05$) in Fig. 4 are not included in Fig. 5b. Abbreviations of land cover classes are explained in the legend of Fig. 1c.

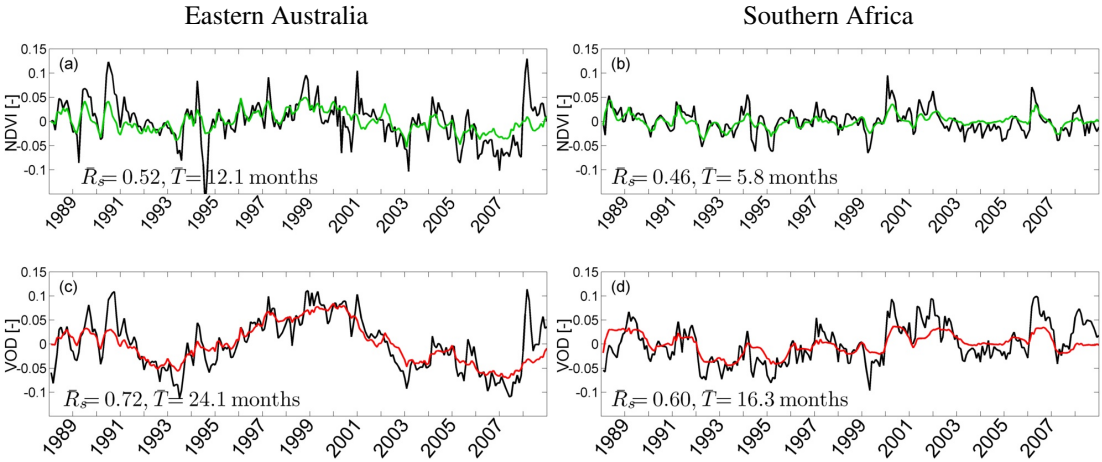

Fig. 6. Time series of expected and observed vegetation anomalies. Parts (a) and (b) show the expected NDVI (green) and observed NDVI (black) vegetation anomalies for regions in eastern Australia (25-30°S, 145-150°E) and southern Africa (25-30°S, 20-25°E), respectively. Parts (c) and (d) are as (a) and (b) except for the expected VOD (red) and observed VOD (black) vegetation anomalies. The average Spearman's ranked correlation coefficient (R_s) and averaging period (T) of all 0.25° resolution grid cells in each 5° region are listed in each sub-plot. Locations of both 5° regions are shown in Fig. 3d.

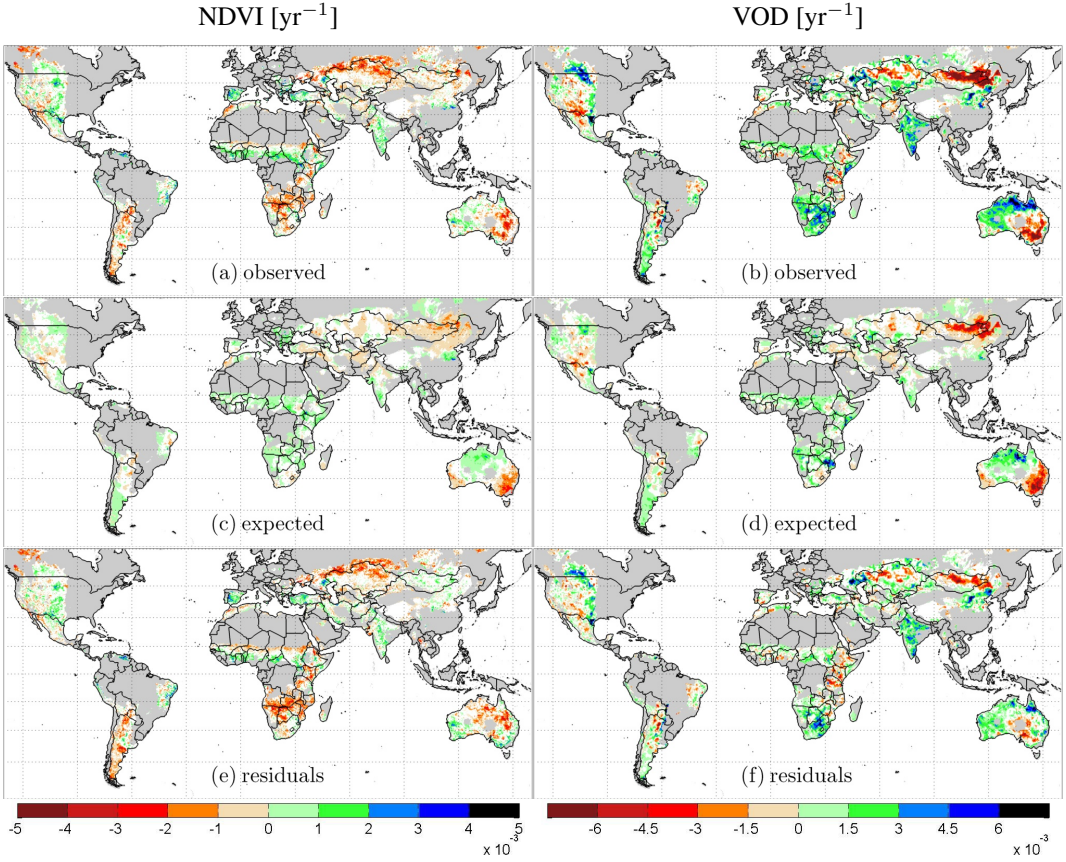

Fig. 7. Linear trends (1988-2008) of the observed, expected and residual for both vegetation indices. Parts (a) and (b) are the NDVI and VOD observed trends, respectively; (c) and (d) are the NDVI and VOD expected trends, respectively; and (e) and (f) are the NDVI and VOD residual trends, respectively. Grid cells with over 60% missing values or without significant trends (p >0.05) are masked (white).

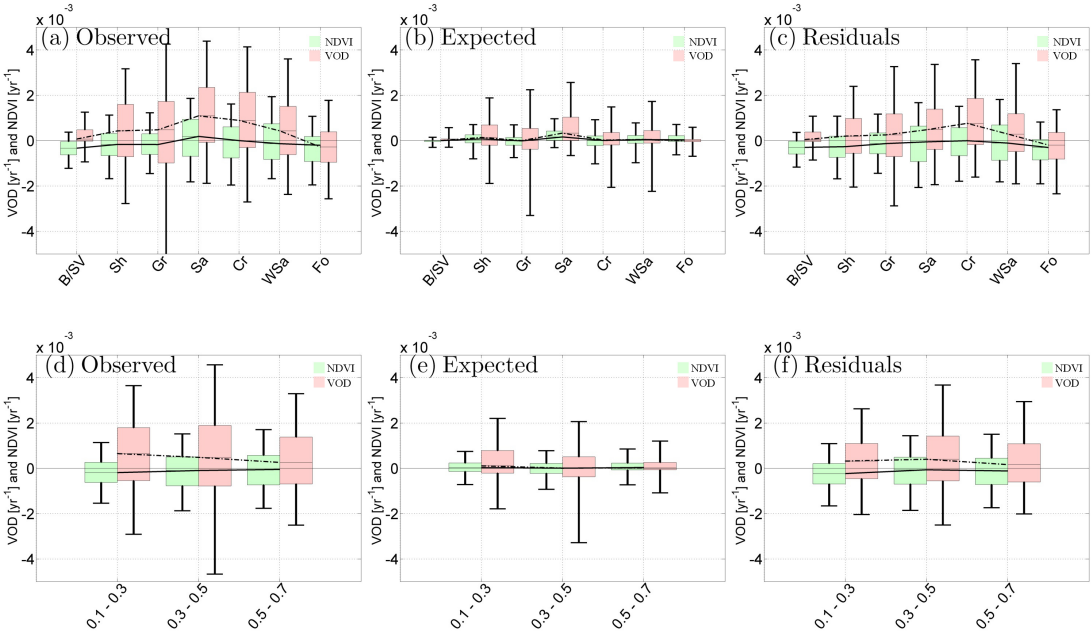

Fig. 8. Box plots of the distribution of observed, expected and residual linear trends for both vegetation indices. Parts (a) and (d) are the observed trends stratified by the land cover and humidity classes, respectively; (b) and (e) are the expected trends stratified by the land cover and humidity classes, respectively; and (c) and (f) are the residual trends stratified by the land cover and humidity classes, respectively. Solid lines indicate the NDVI medians and dash-dot lines the VOD medians. The maximum and minimum extents of the colored boxes indicate 25th and 75th percentiles and whiskers represent the 5th and 95th percentiles. Grid cells with over 60 % missing values are not included in this figure. Abbreviations of land cover classes are explained in the legend of Fig. 1c.

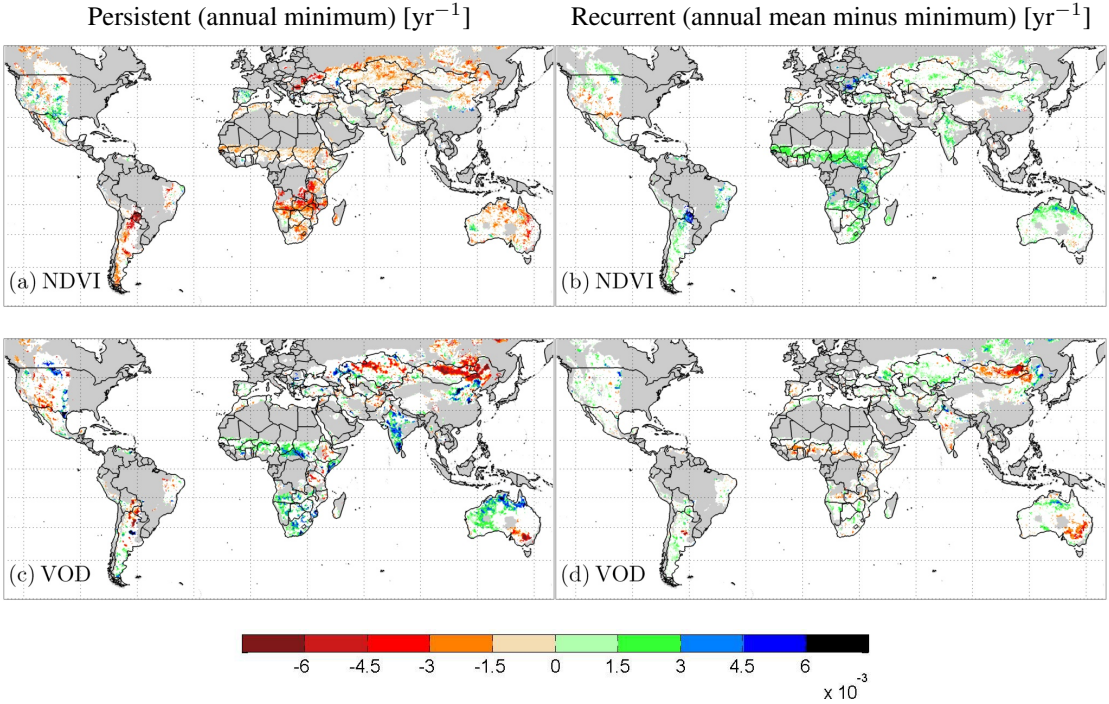

Fig. 9. Long-term (1988-2008) linear trends of the persistent and recurrent components for both vegetation indices. Part (a) shows the NDVI persistent trend; (b) the NDVI recurrent trend; (c) the VOD persistent trend; and (d) the VOD recurrent trend. Grid cells with over 60% missing values or without significant trends (p >0.05) are masked (white).

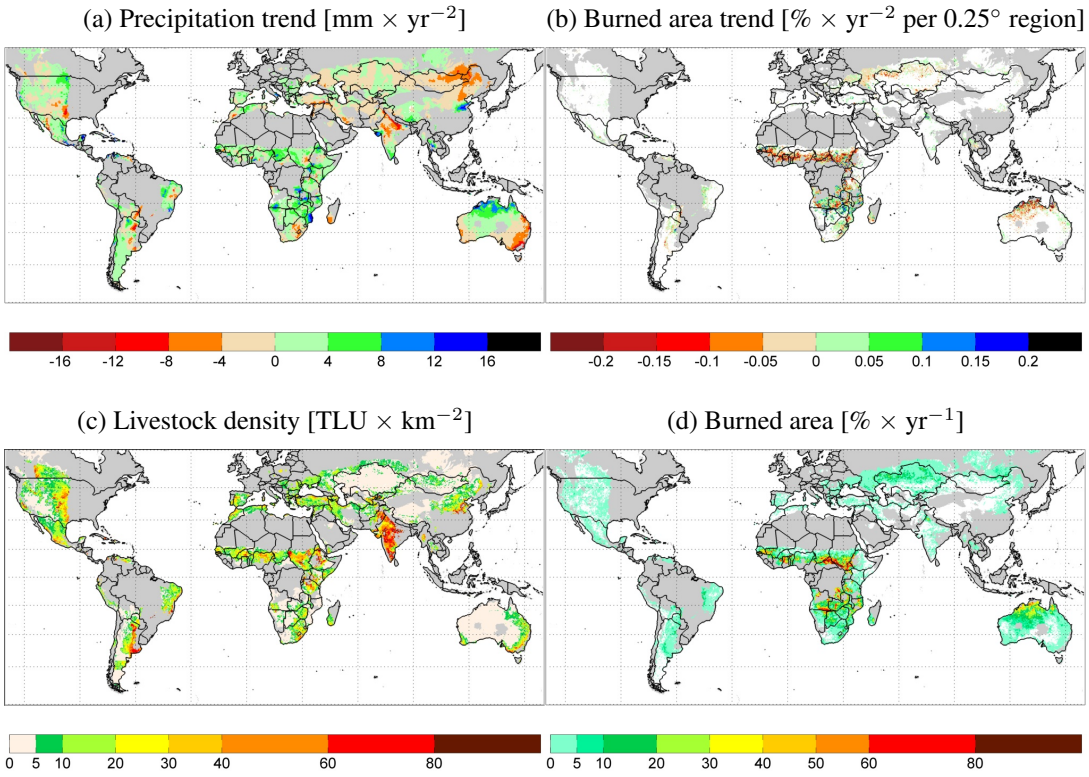

Fig. 10. Datasets used for interpretation of vegetation dynamics. Part (a) linear trend in annual mean precipitation (1988-2008); part (b) linear trend in annual mean burned area (2001-2011); part (c) livestock density; and part (d) mean annual burned area (2001-2011). Due to MODIS data limitations the burned area trends are calculated from 2001-2011. Trends in burned area were only calculated for grid cells with burned area in at least 6 out of 11 years, remaining grid cells are shown in white. For mean burned area (d), grid cells with no fire occurence (mean is zero) are shown in white. Trends are shown for all significance levels.

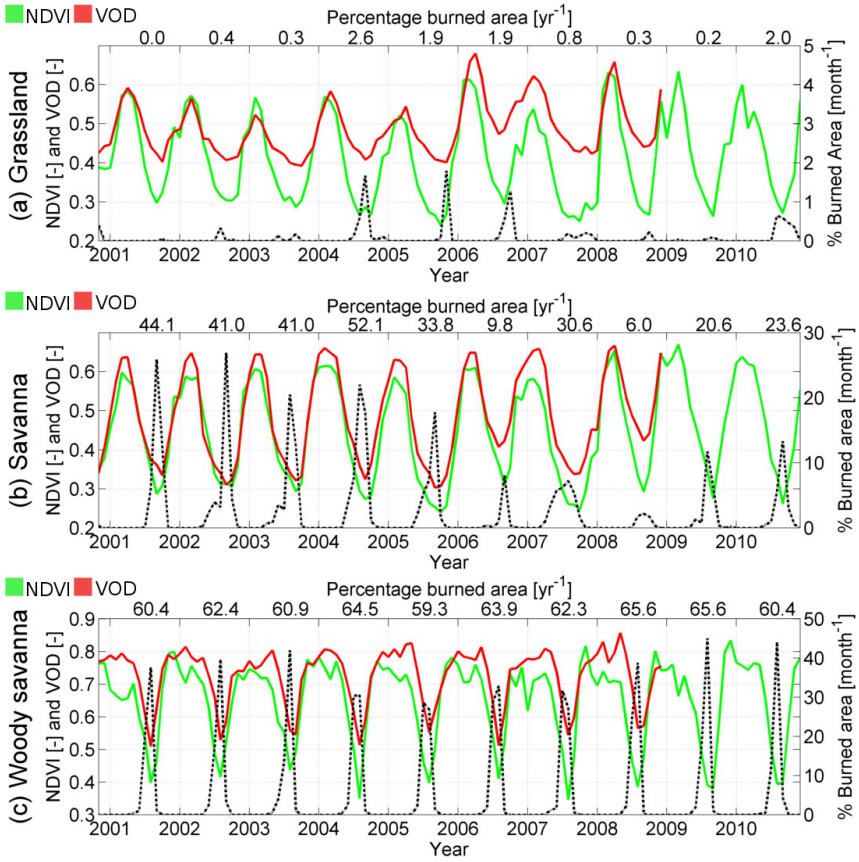

Fig. 11. Time series of NDVI, VOD and burned area (black, dashed) for three selected 0.5° regions with different land cover in southern Africa. Part (a) grassland (19.5-20.0°S,17.0-17.5°E); part (b) savanna (17.0-17.5°S,17.0-17.5°E); and part (c) woody savanna (9.5-10.0°S,19.5-20.0°E). Numbers above the sub-parts are the total burned area [% × yr^{-1}], and locations of study areas are shown as black dots (marked a,b and c) within Fig. 3d.

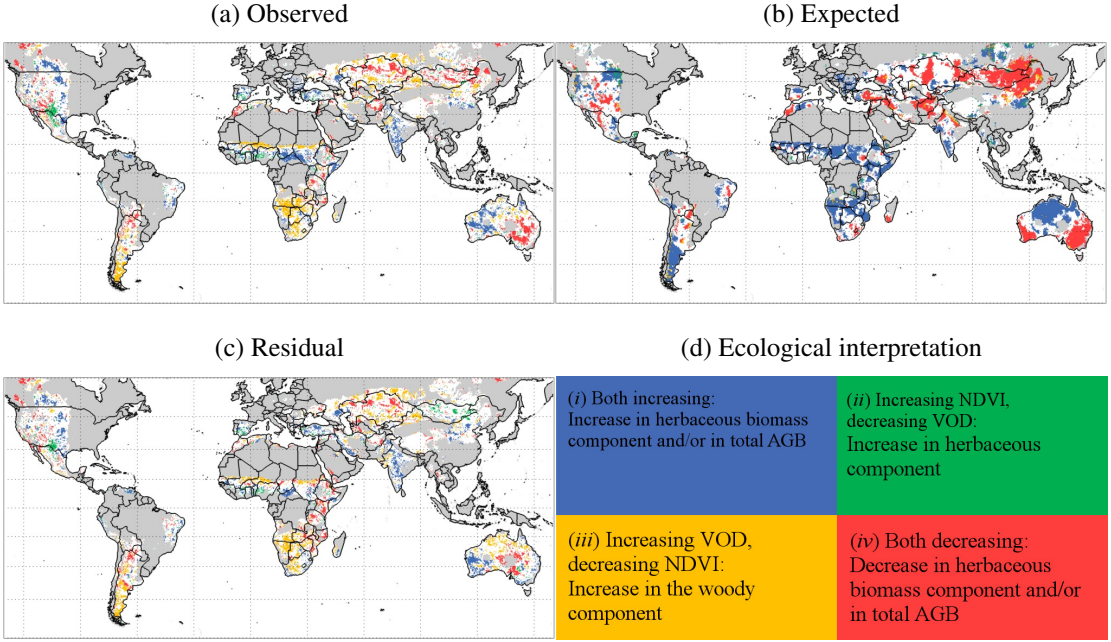

Fig. 12. Co-relationship of NDVI and VOD trends stratified into four classes: (i) both increasing; (ii) increasing NDVI and decreasing VOD; (iii) increasing VOD and decreasing NDVI; and (iv) both decreasing. Part (a) is the observed trends; (b) the expected trends; and (c) the residual trends. Only grid cells with significant trends (p <0.05) and less than 60% missing values in both products are shown. Part (d) shows the ecological interpretation, based on the four expectations of the background theory section.

Table 1. Percentage of global drylands with significant (p<0.05) correlation between API and the two vegetation indices for land cover and humidity classes. The average humidity (P/ET_p) for each land cover class is shown in brackets with the land cover classes ordered in increasing humidity. 1% represents ≈ 750 grid cells (0.25° resolution), abbreviations of land cover classes are explained in the legend of Fig. 1c.

Land cover				Humidity			
Class	Total [%]	NDVI [%]	VOD [%]	Class	Total [%]	NDVI [%]	VOD [%]
B/SV (0.08)	12.7	7.1	8.4	0-0.1	12.2	6.7	8.2
Sh (0.31)	12.0	10.4	10.5	0.1-0.3	17.2	15.8	16.2
Gr (0.42)	14.1	11.6	11.8	0.3-0.5	13.4	11.9	11.8
Sa (0.60)	7.6	5.9	6.4	0.5-0.7	14.4	8.8	8.4
Cr (0.70)	15.7	10.3	9.1	0.7-0.9	14.5	6.6	6.1
WSa (0.81)	9.5	5.4	5.5	0.9-1.1	11.9	4.5	3.9
M/DF (0.93)	12.4	3.8	3.3	1.1-1.3	7.2	2.1	2.0
ENF (1.09)	5.9	1.1	1.3	>1.3	9.1	3.2	2.8
EBF (1.39)	10.0	4.0	3.1				
Total	100.0	59.7	59.4	Total	100.0	59.7	59.4

Appendix A

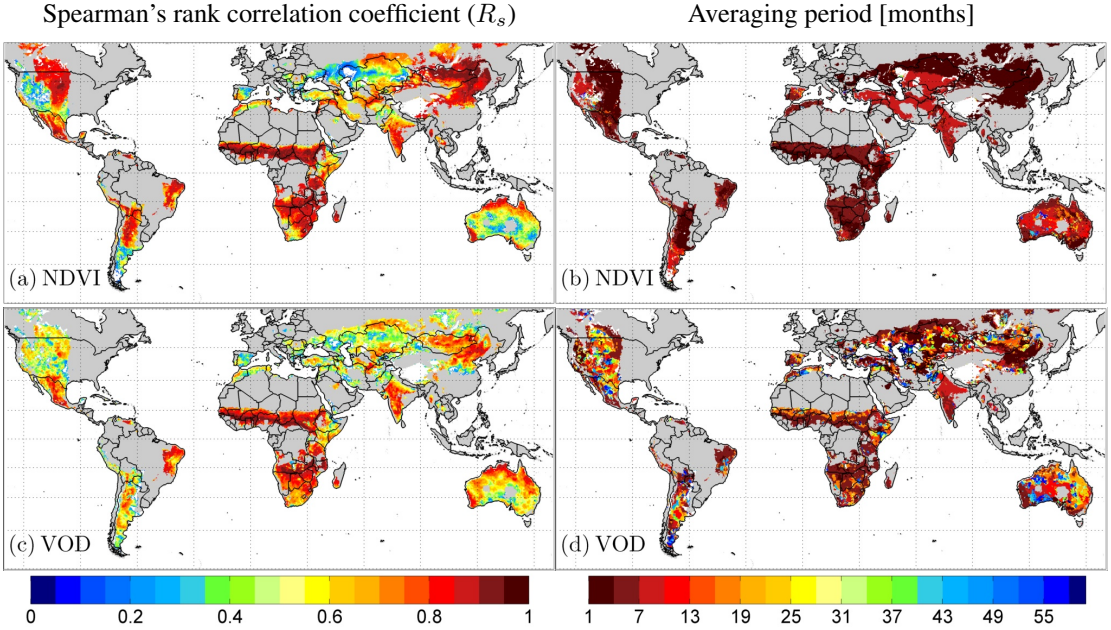

Fig. A.1. Spearman's rank correlation coefficient (R_s) and averaging periods for the two vegetation indices. For the NDVI (a) is the R_s between API and the NDVI and (b) is the averaging period for antecedent precipitation that leads to the highest R_s between PRM and the NDVI. Parts (c) and (d) are as (a) and (b) except for the VOD. Grid cells without significant correlation (p >0.05), with over 60 % missing values, or with a negative correlation coefficients are masked (white).